American Mineralogist, Volume 87, pages 277–292, 2002

Polysomatism in högbomite: The crystal structures of 10*T*, 12*H*, 14*T*, and 24*R* polysomes

CLIVIA HEJNY AND THOMAS ARMBRUSTER*

Laboratorium für chemische und mineralogische Kristallographie, Universität Bern, Freiestr. 3, CH-3012 Bern, Switzerland

ABSTRACT

Högbomite is a closest-packed polysomatic mineral composed of spinel, $T_2M_4O_8$, and nolanite-like, $TM_4O_7(OH)$, modules where T stands for tetrahedrally and M for octahedrally coordinated cations. The modules are stacked in an ordered fashion in various ratios. Single-crystal X-ray diffraction for a 24*R* and a 10*T* polysome and structure modeling for a 12*H* and 14*T* polysome have been applied to characterize different stacking variants.

Högbomite from a spinel-phlogopite schist at Corundum Creek (South Australia) with composition $Mg_{3.8}Fe_{3.2}Zn_{1.6}Ti_{1.0}Al_{18.3}O_{38}(OH)_2$ is a 10*T* polysome with $a = 5.723(1)$, $c = 23.026(4)$ Å, space group $P\bar{3}m1$, $Z = 1$. This polysome with the general formula $T_8M_{20}O_{38}(OH)_2$ is composed of an alternation of spinel (*S*) and nolanite-like (*N*) blocks stacked in the sequence *NSSNS*.

Högbomite from a Fe-Ti deposit at Liganga (Tanzania) with composition $Mg_{13.5}Fe_{5.6}(Zn,Mn,Ni)_{0.2}Ti_{4.7}Al_{41.7}(Cr,Ga)_{0.2}O_{90}(OH)_6$ is a 24*R* polysome with $a = 5.7145(7)$, $c = 55.056(5)$ Å, space group $R\bar{3}m$, $Z = 1$. The structure with the general formula $T_{18}M_{48}O_{90}(OH)_6$ is composed of a periodic alternation of two *S* and two *N* blocks.

The crystal structures of högbomite-12*H*, $T_{10}M_{24}O_{46}(OH)_2$, $a = 5.7$, $c = 27.6$ Å, space group $P6_3mc$, $Z = 1$, and högbomite-14*T*, $T_{12}M_{28}O_{54}(OH)_2$, $a = 5.7$, $c = 32.2$ Å, space group $P\bar{3}m1$, $Z = 1$, were modeled from the stacking principles of the known 6*T*, 8*H*, 10*T*, and 16*H* polysomes. The 12*H* and the 14*T* polysomes have stacking sequences *NSSNSS* and *NSSSNSS*, respectively.

INTRODUCTION

The högbomite-mineral group comprises complex Al-Mg-Fe-Zn-Ti-oxides with a closest-packed oxygen array where the various group members have different oxygen stacking sequences. Crystal structures have been determined for högbomite-8*H* (Gatehouse and Grey 1982), zincohögbomite-8*H* (Armbruster 1998), and zincohögbomite-16*H* (Armbruster et al. 1998). In this nomenclature (Peacor 1967) the suffix n*R*, n*H*, and n*T* stands for n oxygen layers of ca. 2.3 Å thickness and *R*, *H*, or *T* for rhombohedral, hexagonal, or trigonal symmetry. The structure of högbomite has been explained in terms of two different modules, a spinel (*S*) and a nolanite (*N*) module (Gatehouse and Grey 1982; Armbruster 1998; Armbruster et al. 1998). The cubic closest-packed spinel module is composed of a layer with octahedrally coordinated cations (M), labeled **O**-layer, and a layer of tetrahedrally (T) and octahedrally (M) coordinated cations, labeled $\mathbf{T_2}$-layer (Fig. 1). The **O**-layer has composition M_3O_4 and the $\mathbf{T_2}$-layer has composition T_2MO_4. Thus, a complete spinel module, composed of one **O**- and one $\mathbf{T_2}$-layer, has $T_2M_4O_8 = 2 \times TM_2O_4$ stoichiometry. For högbomite the spinel module has composition $MgAl_2O_4$, whereas for zincohögbomite the spinel module is equivalent to gahnite, $ZnAl_2O_4$. For Fe-rich högbomite the spinel module corresponds to hercynite, $FeAl_2O_4$. In the spinel module the octahedral positions are ideally occupied by Al and the tetrahedral positions by Mg, Zn, or Fe^{2+}. The nolanite module is composed of a $\mathbf{T_1}$-layer and an **O**-layer that is very similar to the one in spinel. One anion that links the **O**- and the $\mathbf{T_1}$-layers is an OH group that is assigned to the $\mathbf{T_1}$-layer. The composition of the $\mathbf{T_1}$-layer is $TMO_3(OH)$ and hence the stoichiometry of the nolanite module is $TM_4O_7(OH)$. The nolanite subunit in högbomite has essential Ti^{4+} that may either reside on the octahedral sites of the $\mathbf{T_1}$-layers (högbomite-8*H*: Gatehouse and Grey 1982; zincohögbomite-8*H*: Armbruster 1998) or in the **O**-layers as suggested for zincohögbomite-16*H* (Armbruster et al. 1998). A very simplified formula for a nolanite module in högbomite may be written as $(Mg,Fe^{2+},Zn)Ti(Al,Fe^{3+})_3O_7(OH)$.

The packing of the oxygen layers in nolanite is characterized by alternating cubic (ABC) and hexagonal (ABA) packing, so that each nolanite module is associated with one intercalated oxygen layer of hexagonal closest-packed type. An alternative description of the oxygen stacking sequence uses the symbols "*c*" and "*h*" where "*c*" indicates that a specific oxygen layer has neighboring layers stacked in the cubic closest-packed fashion (ABC). Correspondingly, "*h*" stands for a layer where the layers above and below are of the same stacking type (e.g., the sequence is BCB or BAB). This latter nomenclature is very helpful to indicate the predominance of cubic closest-packed sequences and to assign the $\mathbf{T_1}$ cation layers, which are between "*ch*" type sequences. In addition, the number of "*h*" layers and correspondingly the number of $\mathbf{T_1}$ layers is responsible for the ratio of octahedral to tetrahedral sites in högbomites and for the number of hydroxyl ions.

The substitution of Ti^{4+} by Sn^{4+} in the nolanite-like module links högbomite group minerals to the closely related nigerite group. In nigerite (nigerite-6*T*: Arakcheeva et al. 1995; nigerite-24*R*: Grey and Gatehouse 1979) the octahedral position of the

---

* E-mail: armbruster@krist.unibe.ch

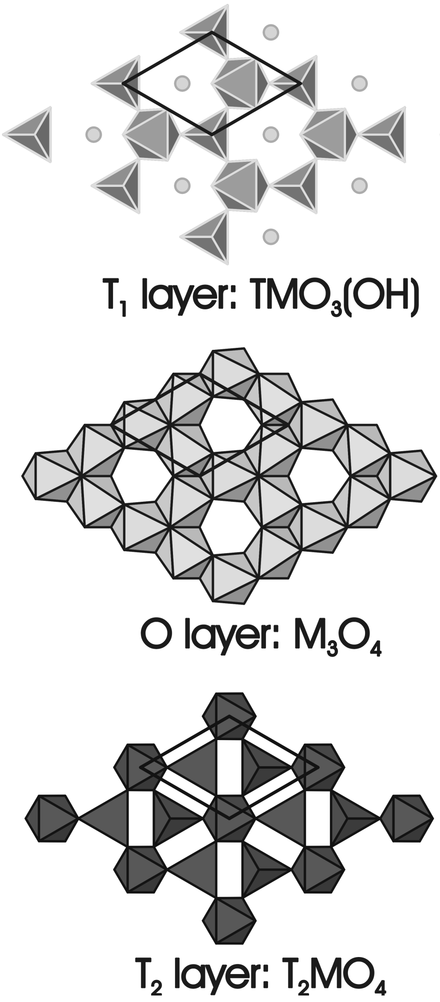

FIGURE 1. Polyhedral model with unit-cell outlines of the $\mathbf{T_1}$-, $\mathbf{T_2}$-, and **O**-layers. In the $\mathbf{T_1}$-layer one quarter of the octahedral sites (1 of 4) and one eighth of the tetrahedral sites (1 of 8) are occupied, resulting in one octahedral and one tetrahedral cation per layer in the unit cell. Circles represent H positions. The formula of the $\mathbf{T_1}$-layer is $TMO_3(OH)$. In the $\mathbf{T_2}$-layer one quarter of the octahedral sites (1 of 4) and one quarter of the tetrahedral sites (2 of 8) are occupied, yielding one octahedral and two tetrahedral cations in the $\mathbf{T_2}$-layer and the formula T_2MO_4. In the octahedral layer three of four octahedral sites are occupied resulting in the formula M_3O_4. A spinel module composed of one **O**- and one $\mathbf{T_2}$-layer has $T_2M_4O_8$ composition and the nolanite module composed of one **O**- and one $\mathbf{T_1}$-layer has $TM_4O_7(OH)$ composition.

$\mathbf{T_1}$-layer in the nolanite module is occupied by Sn and the spinel module is equivalent to gahnite, $ZnAl_2O_4$, or hercynite, $FeAl_2O_4$. Pengzhizongite-6*T* (Chen et al. 1989) is composed of an Sn-nolanite module and an Mg-spinel, $MgAl_2O_4$, module. Note that the trigonal symmetry $P\overline{3}m1$ for the six-layer polysomes requires the suffix 6*T* and not 6*H* as originally assigned to nigerite and pengzhizongite (Arakcheeva et al. 1995; Chen et al. 1989).

Related to the above minerals are the minerals taaffeite-8*H*, $BeMg_3Al_8O_{16}$, musgravite-18*R*, $BeMg_2Al_6O_{12}$, (Nuber and Schmetzer 1983), and pehrmanite, $BeFe^{2+}{}_2Al_6O_{12}$, (Burke and Lustenhouwer 1981) with a corresponding stacking of spinel and nolanite-like modules. However, Be occupies additional tetrahedral voids in the $\mathbf{T_1}$ layer. In högbomite, nigerite, and pengzhizongite these sites are vacant and provide space for a hydroxyl ion. Thus taaffeite, musgravite, and pehrmanite do not contain hydroxyl. The modified $\mathbf{T_1}$ layer in these Be-bearing minerals has been labeled $\mathbf{T_1'}$ (Nuber and Schmetzer 1983).

The following common principles have been observed in the refined structures of högbomite- and nigerite-group minerals. (1) The oxygen atoms are closest-packed. (2) **O**- and $\mathbf{T_x}$-layers alternate. (3) $\mathbf{T_2}$-layers occur between cubic closest-packed oxygen layers, *c*-$\mathbf{T_2}$-*c*. (4) $\mathbf{T_1}$-layers occur on the interface where cubic closest-packing is interrupted by hexagonal closest- packed oxygen layers, *c*-$\mathbf{T_1}$-*h*. (5) Octahedron-octahedron-articulation in the spinel module occurs by edge sharing only but by both corner and edge sharing in the nolanite module. (6) Tetrahedron-tetrahedron articulation occurs by corner sharing in the spinel and the nolanite module (in the $\mathbf{T_1}$-layer the empty tetrahedron is not occupied by cations because of edge sharing of the tetrahedron with adjacent octahedral sites in the **O**-layers). (7) The "empty" tetrahedron in the $\mathbf{T_1}$-layer is occupied by a hydrogen atom.

In högbomite-8*H* (Gatehouse and Grey 1982) and zincohögbomite-8*H* (Armbruster 1998) a nolanite module ($\mathbf{T_1}$-**O**) is followed by a spinel module ($\mathbf{T_2}$-**O**) yielding the sequence *NSNS*. In zincohögbomite-16*H* a nolanite module ($\mathbf{T_1}$-**O**) is followed by three spinel modules ($\mathbf{T_2}$-**O**-$\mathbf{T_2}$-**O**-$\mathbf{T_2}$-**O**) yielding *NSSSNSSS* (Table 1). Although in högbomites and zincohög-bomites the spinel modules have the same geometric appearance, they differ in chemistry, as explained above. The end-member compositions are therefore $Mg_6Al_{14}Ti_2O_{30}(OH)_2$ for högbomite-8*H*, $Zn_6Al_{14}Ti_2O_{30}(OH)_2$ for zincohögbomite-8*H*, and $Zn_{14}Al_{30}Ti_2O_{62}(OH)_2$ for zincohögbomite-16*H*. This clearly demonstrates that zincohögbomite-8*H* and zincohögbomite-16*H* are not polytypes, as pointed out by Armbruster (1998). Due to the different ratio of *S* and *N* modules the stoichiometry is different. Zincohögbomite-8*H* (2*N*2*S*) and zincohögbomite-16*H* (2*N*6*S*) are in fact so called polysomes. In högbomite-8*H* (2*N*2*S*) and högbomite-24*R* (6*N*6*S*) the same ratio of *S* and *N* modules is present and hence they may qualify as polytypes.

Due to the unknown number of OH groups and the unidentified type of polysome the chemical formulas for various högbomites have been normalized to different numbers of oxygen atoms or cations (Petersen et al. 1989). The above principle of building up the structures of högbomite polysomes from different modules (Table 1) allows for each polysome the true stoichiometry or formula to be calculated (Armbruster 1998).

McKie (1963) used X-ray single-crystal methods to determine the stacking periodicity in högbomites from seven different occurrences. He determined polysomes that he regarded as polytypes with a periodicity of 8, 10, 12, 30, and 36 oxygen layers. Notice that McKie (1963) used a different nomenclature from that of Peacor (1967), and we use the latter in this paper. In addition, McKie (1963) observed disordered polysomes characterized by streaked reflections parallel to c^*. A macroscopic högbomite "single-crystal" may be composed of

TABLE 1. Oxygen stacking sequences and modular composition of högbomite polysomes and related structures

Suffix	Space group	Sequence of cubic “*c*” and hexagonal “*h*” closest packed oxygen layers	Sequence of spinel (*S*) * and nolanite (*N*) * modules	Sum of spinel (*S*) and nolanite (*N*) modules	Theoretical composition	Name and reference
4*H*	$P6_3mc$	*chch*	*NN*	2*N*	$2 \times TM_4O_7(OH)$	nolanite†
6*T*	$P\bar{3}m1$	2 × (*c* + *ch*)	*NNS*	2*N*1 *S*	$2 \times T_2M_6O_{11}(OH)$	nigerite ‡
8*H*	$P6_3mc$	2 × (*cc* + *ch*)	*NSNS*	2*N*2 *S*	$2 \times T_3M_8O_{15}(OH)$	högbomite§ zincohögbomite‖ taaffeite #
10*T*	$P\bar{3}m1$	2 × (*ccc* + *ch*)	*NSSNS*	2*N*3 *S*	$2 \times T_4M_{10}O_{19}(OH)$	högbomite **
12*H*	$P6_3mc$	2 × (*cccc* + *ch*)	*NSSNSS*	2*N*4 *S*	$2 \times T_5M_{12}O_{23}(OH)$	modeled **
14*T*	$P\bar{3}m1$	2 × (*ccccc* + *ch*)	*NSSSNSS*	2*N*5 *S*	$2 \times T_6M_{14}O_{27}(OH)$	modeled **
16*H*	$P6_3mc$	2 × (*cccccc* + *ch*)	*NSSSNSSS*	2*N*6 *S*	$2 \times T_7M_{16}O_{31}(OH)$	zincohögbomite ††
18*R*	$R\bar{3}m$	3 × (*cc* + *chhc*)	3 × (*NNS*)	6*N*3 *S*	$6 \times T_2M_6O_{11}(OH)$	musgravite #
24*R*	$R\bar{3}m$	3 × (*cccc* + *hcch*)	3 × (*NNSS*)	6*N*6 *S*	$6 \times T_3M_8O_{15}(OH)$	nigerite ‡‡ högbomite **
30*R*	$R\bar{3}m$	3 × (*cccccc* + *hcch*)	3 × (*NNSSS*)	6*N*9 *S*	$6 \times T_4M_{10}O_{19}(OH)$	predicted
36*R*	$R\bar{3}m$	3 × (*cccccccc* + *hcch*)	3 × (*NNSSSS*)	6*N*12 *S*	$6 \times T_5M_{12}O_{23}(OH)$	predicted

* $N = \mathbf{O-T_1}$, $S = \mathbf{O-T_2}$.

† Gatehouse et al. 1983.

‡ Arakcheeva et al. 1995.

§ Gatehouse and Grey 1982.

‖ Armbruster 1998.

Nuber and Schmetzer 1983; for taaffeite and musgravite: no hydroxyl group, Be instead of H.

** This study.

†† Armbruster et al. 1998.

‡‡ Grey and Gatehouse 1979.

several polysomes, which was confirmed by Bovin (1981) in a high-resolution transmission electron microscope study. In addition to the stacking variants reported by McKie (1963), högbomite-24*R* (Schmetzer and Berger 1990) and zincohögbomite-16*H* (Armbruster et al. 1998) were identified. For Sn-rich and Ti-poor nigerite, only 6*T* and 24*R* polysomes are known (e.g., Neiva and Champness 1997). The structure of musgravite, $BeMg_2Al_6O_{12}$, exhibits stacking of an 18*R* polysome (Nuber and Schmetzer 1983). Only even numbers of oxygen layers are possible in these polysomatic series because both the spinel and the nolanite module are composed of two oxygen layers.

There are still several problems associated with högbomite. (1) We are not aware of any experimental study reporting stability relations. (2) The relation between type of polysome and chemical composition is not clear, although it has been suggested that the concentration of Ti^{4+} plays an important role (e.g., Petersen et al. 1989). To shed light on the latter problem it is important to learn more about högbomite samples where chemistry and type of polysome have been determined. For this reason we surveyed several högbomite samples described in the literature to find new polysomes and to elucidate the relation between structure and chemistry. If the structural principles are understood it is also possible to model the structures of högbomite polysomes that were not found. Thus, modeling of polysome structures is an additional goal of this study.

SAMPLE DESCRIPTION

Högbomite-24*R*

The högbomite-24*R* crystals originate from a Fe-Ti-deposit at Liganga (Tanzania). The högbomite-bearing sample was kindly supplied by M.A. Zakrzewski, who described the petrology of the host rock and discussed the petrogenesis and geochemistry of these materials (Zakrzewski 1977). Besides chlorite and spinel, högbomite occurs as a gangue mineral in the ore-body, which is situated in an anorthosite-massif. Sample material comes from a part of the deposit where magnetite is extensively replaced by hematite and högbomite is the main gangue mineral.

Zakrzewski (1977) distinguished three types of högbomite occurrences. Högbomites of secondary origin are formed from spinel by exchange of (Mg + Zn) with Ti, while loss of Al is balanced by oxidation of Fe. These högbomites are fine-grained and are either partly euhedral and overgrowing spinel or occur as rounded aggregates. The latter högbomites were assumed to represent polysomes with a 10-layer repeat sequence (Zakrzewski 1977). In addition, there are also primary euhedral crystals. These occur in contact with magnetite-ilmenite, between magnetite crystals, or within magnetite. Euhedral crystals with high Ti content were used in this study.

Högbomite-10*T*

Allen Pring kindly provided a sample containing högbomite-10*T* crystals. The sample originates from Corundum Creek, in the Mount Painter Province of South Australia, as described by Teale (1980). Högbomite is present as millimeter sized grains in a spinel-phlogopite schist with phlogopite and spinel as the dominant phases plus additional corundum, rutile, zircon, and monazite. The host rock formed during two prograde upper amphibolite facies metamorphic events (Teale 1980). The primary phlogopite-spinel-taaffeite assemblage developed during an initial high-grade metamorphic event. Högbomite formed at the expense of spinel and taaffeite during a second metamorphic event. Our sample did not reveal any taaffeite, but wagnerite, Mg_2PO_4F, was identified as an additional phase.

In thin-section both samples form tabular translucent crystals of honey to dark reddish-brown color. Under crossed polarizers the crystals are distinctly anisotropic and can be discriminated from spinel. Macroscopically the crystals are brown with metallic to adamantine luster. In reflected light högbomite appears gray and slightly lighter than spinel and shows orange to reddish-brown internal reflections.

EXPERIMENTAL METHODS

Electron microprobe analyses and FTIR spectrometry

Minerals were analyzed with a Cameca SX-50 microprobe using beam conditions of 15 kV and 14 nA, wavelength-dispersive spectrometers, and when possible, an enlarged spot size of ca. 10 μm. Natural and synthetic minerals were used as standards: corundum Al*K*α (TAP), spinel Mg*K*α (TAP), ilmenite Ti*K*α (PET), almandine Fe*K*α (LiF), gahnite Zn*K*α (LiF), escolaite Cr*K*α (LiF), tephroite Mn*K*α (LiF), SnS_2 Sn*K*α (LiF), NiO Ni*K*α (LiF), $HgGa_2S_4$ Ga*K*α (LiF), anorthite Ca*K*α (PET), phlogopite F*K*α (TAP), scapolite Cl*K*α (PET). Raw data were processed with the Cameca version of the PAP (Pouchou and Pichoir 1991) routine. Fourteen electron-microprobe analyses were collected for several grains of högbomite-24*R* from Liganga to examine chemical homogeneity. For högbomite-10*T* a thick section of the host rock and three single crystals embedded in resin and polished were measured.

In order to prove the presence of hydroxyl ions an FTIR spectrum of a högbomite-10*T* single crystal positioned on an aperture of 100 mm diameter was recorded between 600 and 8000 cm^{-1} with a Perkin Elmer FTIR spectrometer 1760× equipped with a Perkin Elmer IR microscope and a liquid nitrogen cooled MCT detector.

Crystal-structure analyses

A single crystal of the Liganga högbomite, ca. 50 × 50 × 140 μm^3 in size, was drilled out of a polished thick-section using the micro-drilling device of Medenbach (1986). Hexagonal cell parameters of $a = 5.7145(7)$ and $c = 55.056(5)$ Å obtained from 10 reflections with $8.9 < \theta < 25.5$ collected on a ENRAF NONIUS CAD4 diffractometer (Mo*K*α radiation), led to the identification of the 24*R* polysome of högbomite. A rotation photograph around the **c**-axis was recorded to eliminate the possibility of weak interlayer reflections. Diffraction data were collected with graphite-monochromated Mo*K*α radiation up to $\theta = 30°$, yielding 3779 reflections of which 1314 were unique and 908 had $F > 4\sigma(F)$. Data reduction, including background and Lorentz polarization correction, was carried out with the SDP program system (Enraf Nonius 1983). An empirical absorption correction using the ψ-scan technique was applied. Experimental details of data collection and structure refinement are summarized in Table 2. Systematic absences for the 24*R* polysome indicated $R\bar{3}m$, $R\bar{3}$, $R32$, $R3m$, or $R3$ as possible space groups. By analogy with nigerite-24*R* (Grey and Gatehouse 1979) space group $R\bar{3}m$ was chosen. The positions of cations and oxygen atoms were found by direct methods using the program SHELXS-97 (Sheldrick 1997a). Structure refinement was performed with the program SHELXL-97 (Sheldrick 1997b). The hydrogen atom appeared in subsequent difference-Fourier maps and the O2-H distance (OH group) was restrained at 0.90(5) Å in the last refinement cycles.

A crystal of högbomite-10*T* (50 × 70 × 90 μm^3) from Corundum Creek was hand picked from the rock sample. Hexagonal cell parameters of $a = 5.723(1)$, $c = 23.026(4)$ Å were measured with a three-circle Siemens SMART system equipped with a CCD area detector, which led to the identification of the 10*T* polysome. Diffraction data were collected at room temperature up to $\theta = 28°$ using graphite-monochromated Mo*K*α radiation. Of the 3753 reflections collected 651 were unique and 504 had $F > 4\sigma(F)$. Experimental details of data collection and structure refinement are summarized in Table 3. Data reduction, including Lorentz and polarization corrections, was performed with the SAINT+ program (Bruker AXS 1999). Empirical absorption correction using the ψ-scan technique was applied using the program XPREP (Bruker AXS 1997), which reduced *R*(int) from 4.75 to 3.71%. Systematic absences for the 10*T* polysome allowed for 16 possible space groups of trigonal and hexagonal symmetry. The lowest symmetry space group was *P*3 and in this trial space group the structure was determined by direct methods (SHELXS-97, Sheldrick 1997a) and

TABLE 2. Details of X-ray data collection and refinement for högbomite-24*R*

Space group	$R\bar{3}m$ (no. 166)
a, *c* (Å)	5.7145(7), 55.056(5)
V ($Å^3$)	1557.0(3)
Diffractometer	Enraf Nonius CAD4
X-ray radiation	graphite-monochromated Mo*K*α
X-ray power (kV/mA)	55/40
Temperature (K)	293
Crystal size (μm^3)	50 × 50 × 140
Upper θ limit (°)	30
h, *k*, *l* limit	$\bar{1}0 \le h \le 8$, $\bar{1} \le k \le 10$, $\bar{1} \le l \le 99$
μ (mm^{-1})	2.49
Reflections measured	3779
Unique reflections	1314
Reflections $> 4\sigma(F)$	908
Absorption correction	empirical: ψ-scans
R (int)	3.06%
R (σ)	2.85%
Number of least square parameters	43
GooF	1.134
$R1$, $F_o > 4\sigma(F_o)$	3.18%
$R1$, all data	5.89%
w*R* (on F^2)	7.57%

TABLE 3. Details of X-ray data collection and refinement for högbomite-10*T*

Space group	$P\bar{3}m1$ (no. 164)
a, *c* (Å)	5.723(1), 23.026(4)
V ($Å^3$)	653.1(6)
Diffractometer	Siemens SMART CCD system
X-ray radiation	graphite-monochromated Mo*K*α
X-ray power (kV / mA)	50/40
Temperature (K)	293
Crystal size (μm^3)	50 × 70 × 90
Detector to sample distance (cm)	5.521
Upper θ limit (°)	28
Rotation axis	ω
Rotation width (°)	0.15
Total number of frames	2542
Frame size (pixel)	512 × 512
Data collection time per frame (sec)	60
Collection mode	automated full hemisphere
h, *k*, *l* limit	$\bar{7} \le h \le 7$, $\bar{7} \le k \le 7$, $\bar{1}2 \le l \le 28$
μ (mm^{-1})	4.69
Reflections measured	3753
Unique reflections	651
Reflections $> 4\sigma$ (*F*)	504
Absorption correction	empirical: ψ-scans
Twinned by m in {001}	0.534(2)/0.466
R (int)	3.71%
R (σ)	3.74%
Number of least square parameters	56
GooF	0.919
$R1$, $F_o > 4\sigma(F_o)$	2.79%
$R1$, all data	4.11%
w*R* (on F^2)	6.60%

refined with the program SHELXL-97 (Sheldrick 1997b). At this stage it was recognized that the crystal was twinned by a mirror plane perpendicular to the **c**-axis. A mirror plane running through a cation layer, perpendicular to the **c**-axis (in the trial space group $P3$), disturbed the closest oxygen packing. This was intuitively interpreted as an artifact due to twinning perpendicular to a $\overline{3}$-axis. In the next step, structure refinement and difference-Fourier analysis in space group $P\overline{3}$, twinned by a mirror plane perpendicular to **c**, was successfully attempted. This approach led to the identification of all cation and oxygen sites. Finally, structural drawings and parameter correlation were used to derive the true space group $P\overline{3}m1$, for which the final refinements were performed, allowing for twinning as described above. The hydrogen atom appeared in subsequent difference-Fourier maps and the O4-H distance (OH group) was constrained to 0.90(5) Å in the last refinement cycles.

Both crystal structure refinements were performed with scattering factors for neutral atoms (program SHELXL-97, Sheldrick 1997b). Isotropic displacement parameters were refined for all atoms. For the proper assignment of cations to tetrahedrally and octahedrally coordinated sites following strategy was used: (1) In test refinements all isotropic displacement parameters of cation sites were fixed at $U_{\text{iso}} = 0.005$ Å^2, Al scattering curves were assigned, and the populations of the cation sites were allowed to vary. (2) Site multiplicity and refined Al populations allowed the number of scattering electrons to be estimated for each site. (3) If the estimate of electrons for octahedrally coordinated sites was between 12 and 13 the Al scattering curve was retained and the population was fixed at 1.0. If the estimate of electrons for tetrahedrally coordinated sites was between 12 and 13 the Mg scattering curve was introduced and the population was fixed at 1.0. (4) If the estimate of scattering electrons for octahedrally coordinated sites was above 13 a mixed Al-Fe population was assumed and the Al/Fe ratio was allowed to vary in subsequent refinement cycles. For tetrahedrally coordinated sites mixed Mg-Fe populations were refined. (5) For crystal chemical reasons discussed below, Ti was assigned to the octahedral position of the $\mathbf{T_1}$-layer and fixed according to the concentration determined by electron-microprobe analysis. The remaining cations on the Ti-bearing site were assigned to Fe, Mg and allowed to refine. (6) Displacement parameters were allowed to refine. Due to an unfavorable ratio between observations [reflections > $4\sigma(F)$] and least-squares variables for högbomite-24*R*, cation positions of similar occupancy, symmetry, and coordination were subsequently constrained to the same displacement parameter. Due to similar ionic radii and X-ray scattering power Fe and Zn could not be distinguished in the structure refinements. In addition, Mg and Al have similar X-ray scattering power that must be taken into consideration when interpreting X-ray results and comparing them with chemical compositions obtained from electron-microprobe analyses.

Modeling of polysomes with 12 and 14 layer stacking sequence

The structural units of högbomite-polysome construction are (1) cubic and hexagonal closest-packed oxygen layers and (2) spinel- and nolanite-module sequences (Table 1). The polysomes 6*T*, 8*H*, and 10*T* are each composed of two *N* modules. From the 6*T* polysome, which has one *S* module, to the 16*H* polysome the number of *S* modules increases (exceptions are polysomes of rhombohedral symmetry). The 8*H* polysome has two *S* modules and the 10*T* polysome has three *S* modules. The 16*H* polysome is composed of two *N* and six *S* modules. Following this mechanism the gap between the 10*T* and the 16*H* polysome must be filled with a polysome of a 12-layer sequence, that is expected to have two *N* and four *S* modules, and a polysome with a 14-layer sequence, that must have two *N* and five *S* modules. Polysomes with a 12-layer sequence have been reported by McKie (1963) and Ding et al. (1982) but polysomes with a 14-layer sequence have hitherto not been analyzed. An oxygen-packing sequence as indicated in Table 1 was modeled with oxygen layers at $z = n/12$ ($n = 0 - 11$) for the polysome with the 12-layer sequence and with oxygen layers at $z = n/14$ ($n = 0 - 13$) for the 14-layer polysome. Possible octahedrally coordinated sites must be situated at $z = (2n + 1)/24$ and $z = (2n + 1)/28$ for the 12- and the 14-layer polysome, respectively, and possible tetrahedrally coordinated sites at $z = (2n + 1)/48$ for the 12-layer polysome and at $z = (2n + 1)/56$ for the 14-layer polysome. According to the rule that a $\mathbf{T_2}$-layer must be situated between cubic closest-packed oxygen layers and a $\mathbf{T_1}$-layer between cubic and hexagonal closest-packed oxygen layers, the cations were distributed between the oxygen layers, where they are considered to fulfil the criteria for correct polyhedra articulation, as stated by Grey and Gatehouse (1979).

The lattice parameter *a* was assessed for both polysomes as 5.7 Å, and *c* was fixed at 12 × 2.3 = 27.6 Å for the 12-layer repeat polysome and at 14 × 2.3 = 32.2 Å for the 14-layer repeat polysome. All atomic coordinates were calculated in space group $P1$. The structure factors $F(hkl)$ of the predicted structures were subsequently calculated for all reflections up to 42.5°θ using the program FCGEN (1998) with neutral atom-scattering factors for Mo$K\alpha_1$-radiation. The calculated diffraction pattern (in terms of F_{calc}) was submitted to the XPREP program (Bruker AXS 1997). This program was used to explore the extinction rules and to identify symmetry-equivalent reflections. After the true symmetry was found the coordinates were transformed into the correct setting. The correctness of the symmetry was tested by a subsequent structure refinement with F_{calc} as observations. For the correct model such refinements converged to $R1$-values close to 1%. The remaining misfit was due to rounding errors of the coordinates. The 12*H* polysome is acentric and has space group $P6_3mc$ whereas the 14*T* polysome is centric with space group $P\overline{3}m1$.

RESULTS

The chemical compositions for högbomite-24*R* from Liganga and högbomite-10*T* from Corundum Creek are listed in Tables 3 and 4. The formula of högbomite-24*R* was calculated on the basis of 66 cations and of högbomite-10*T* on the basis of 28 cations. The Fe^{2+}/Fe^{3+} ratio (approximately 1:1 for both samples) was calculated to balance 78 [10*T* polysome of $T_8M_{20}O_{38}(OH)_2$ stoichiometry] and 186 [24*R* polysome of $T_{18}M_{48}O_{90}(OH)_6$ stoichiometry] negative charges.

The analyses of högbomite-24*R* are in good agreement with the results for euhedral högbomite (sample 58-4, 58-8, 58-9)

TABLE 4. Electron-microprobe analyses of högbomite-24*R*; chemical formula normalized on 66 cations

	Zakrzewski (1979) Mean (wt%)	Zakrzewski (1979) σ (wt%)	Zakrzewski (1979) Minimum (wt%)	Zakrzewski (1979) Maximum (wt%)	This study Mean (wt%)	This study σ (wt%)	Elements	apfu
MgO	13.25	0.40	14.45	16.55	15.34	0.50	Mg	13.506
MnO	0.13	0.01	0.02	0.13	0.09	0.03	Mn	0.045
NiO			0.06	0.19	0.11	0.05	Ni	0.052
ZnO	0.71	0.10	0.17	0.41	0.34	0.07	Zn	0.148
Al_2O_3	58.89	0.65	58.50	61.37	60.01	0.78	Al	41.769
Fe_2O_3	16.93	0.63	10.66	15.17	12.67	1.25	Fe	5.631
Cr_2O_3	1.02	0.07	0.02	0.47	0.26	0.13	Cr	0.121
Ga_2O_3			0.00	0.29	0.14	0.10	Ga	0.053
TiO_2	10.31	0.09	9.61	11.27	10.52	0.47	Ti	4.672
SnO_2			0.00	0.09	0.01	0.02	Sn	0.002
Sum					99.49		Sum	65.999

Notes: All Fe calculated as Fe_2O_3. In order to balance 186 negative charges [$O_{90}(OH)_6$], as derived from the structure refinement, a Fe^{2+}/Fe^{3+} ratio of 2.920/2.711 has to be assumed.

given by Zakrzewski (1977). The preparation technique of isolated small single crystals (högbomite-10*T*) led to poor sample conductivity. Thus the oxide sums in analyses on isolated single crystals are lower than those in the bulk material. Comparison of the calculated atoms per formula unit of crystals within the host rock and the single crystals embedded in resin showed no difference. The analyzed crystals of högbomite-10*T* are chemically very homogeneous. Nevertheless, the observed composition is different to the one given by Teale (1980). Teale's högbomites have less Fe and Zn but more Mg than the högbomites in this study (Table 5). As A. Pring (who provided the sample) noticed, the rock originates from the area described by Teale (1980), but this area is rather large and contains numerous outcrops. The sample examined in this study is obviously from a different outcrop.

Atomic coordinates of the refined structures of the 24*R* and 10*T* polysomes are given in Tables 6 and 7, those of the modeled polysomes 12*H* and 14*T* in Tables 8 and 9. The stacking sequences of the corresponding structures are displayed in Tables 10 to 13 and Figures 2 to 5. Selected interatomic distances are summarized in Tables 14 and 15. A list of calculated and observed structure factors is deposited as Appendix 1 for högbomite-24*R* and Appendix 2 for högbomite-10*T*.[1]

Structure description

Högbomite-24*R*. This polysome is formed by a periodic alternation of two nolanite-like and two spinel modules, 3x (*NNSS*), leading to the general formula $T_{18}M_{48}O_{90}(OH)_6$. The

TABLE 5. Electron-microprobe analyses (5 points) of the X-rayed crystal of högbomite-10*T* and of several crystals (26) in the host rock

	Single crystal Minimum (wt%)	Single crystal Maximum (wt%)	Single crystal Mean (wt%)	Single crystal σ (wt%)	Several crystals of the sample rock Minimum (wt%)	Several crystals of the sample rock Maximum (wt%)	Several crystals of the sample rock Mean (wt%)	Several crystals of the sample rock σ (wt%)	Teale (1980) no. 1 (wt%)	Teale (1980) no. 2 (wt%)
MgO	9.16	9.47	9.34	0.12	8.61	10.92	9.41	0.76	18.21	19.27
MnO	0.40	0.47	0.42	0.03	0.33	0.49	0.39	0.04		
NiO	0.01	0.04	0.02	0.02	0.00	0.06	0.02	0.02		
ZnO	7.94	9.39	8.17	0.17	5.27	11.50	8.64	1.70	0.53	0.19
FeO	13.89	14.29	14.14	0.16	13.28	16.17	14.73	0.92	9.65	8.91
Al_2O_3	56.57	57.77	57.31	0.48	58.62	60.20	59.52	0.45	65.34	66.42
Cr_2O_3	0.00	0.02	0.01	0.01	0.00	0.14	0.03	0.03		
TiO_2	4.83	4.91	4.88	0.03	4.60	5.29	5.02	0.18	6.44	5.30
SnO_2	0.00	0.03	0.01	0.01	0.00	0.06	0.02	0.02		
Sum			94.30				97.78		100.17	100.09
			Calculated formula							
			apfu				apfu		apfu	apfu
Mg			3.771				3.670		6.471	6.783
Mn			0.097				0.086			
Ni			0.005				0.004			
Zn			1.634				1.669		0.093	0.033
Fe			3.203				3.223		1.924	1.759
Al			18.291				18.352		18.357	18.483
Cr			0.002				0.006			
Ti			0.995				0.988		1.154	0.941
Sn			0.001				0.002			
Sum			27.999				28.000		27.999	27.999

Notes: Calculated formulas were normalized to 28 cations. All Fe calculated as FeO. In order to balance 78 negative charges [$O_{38}(OH)_2$], as derived from the structure refinement, a Fe^{2+}/Fe^{3+} ratio of 1.489/1.714 for the single crystal and 1.602/1.621 for the mean chemical analysis of several crystals has to be assumed. For comparison the two analyses given by Teale (1980) are also listed.

---

[1] For a copy of Appendices 1, 2, 3, and 4, document item AM-02-002, contact the Business Office of the Mineralogical Society of America (see inside front cover of recent issue) for price information. Deposit items may also be available on the American Mineralogist web site at http://www.minsocam.org.

TABLE 6. Final atomic coordinates, populations, and U_{iso} values for högbomite-24*R*, space group $R\bar{3}m$, a = 5.7145(7), c = 55.056(5) Å

Atom	Population		*x*	*y*	*z*	U_{iso}
M1	**O**	1 Al	0	1/2	0	0.0070(2)
M2	$\mathbf{T_1}$	0.78 Ti + 0.17(1) Fe + 0.05 Mg	2/3	1/3	0.04763(1)	0.0043(1)
T3	$\mathbf{T_1}$	0.83(1) Mg/Al + 0.17 Fe	0	0	0.03051(2)	0.0051(2)
M4	**O**	1 Al	0.16818(7)	0.3364(1)	0.08176(1)	0.0049(1)
M5	$\mathbf{T_2}$	1 Al	0	0	0.12479(2)	0.0049(1)
T6	$\mathbf{T_2}$	0.83(1) Mg + 0.17 Fe	1/3	–1/3	0.13483(2)	0.0051(2)
T7	$\mathbf{T_2}$	0.79(1) Mg + 0.21 Fe	–1/3	1/3	0.11271(2)	0.0051(2)
M8	**O**	1 Al	–1/6	1/6	1/6	0.0049(1)
O1			0.8227(2)	0.1773(2)	0.02020(3)	0.0108(3)
O2			1/3	2/3	0.01818(5)	0.0084(5)
O3			0.4995(2)	0.5005(2)	0.06376(3)	0.0089(3)
O4			0	0	0.06397(5)	0.0088(5)
O5			–0.1487(2)	0.1487(2)	0.10311(3)	0.0092(3)
O6			1/3	2/3	0.09942(5)	0.0071(4)
O7			0.1483(2)	–0.7034(3)	0.14714(2)	0.0061(2)
O8			–1/3	1/3	0.14788(5)	0.0070(4)
H			1/3	2/3	0.0335(8)	0. 05(3)

Notes: The refined formula from X-ray analyses is $Al_{42.0}Mg_{15.0}Fe_{4.3}Ti_{4.7}O_{90}(OH)_6$.

TABLE 7. Final atomic coordinates, populations and U_{iso} values for högbomite-10 *T*, space group $P\bar{3}m1$, a = 5.722(1), c = 23.026(4) Å

Atom	Population		*x*	*y*	*z*	U_{iso}
M1	$\mathbf{T_2}$	1 Al	0	0	0	0.0102(9)
T2	$\mathbf{T_2}$	0.77(1) Fe, Zn + 0.23 Mg	1/3	–1/3	–0.02563(7)	0.0073(6)
M3	**O**	1 Al	0.3384(3)	0.1692(2)	–0.10125(6)	0.0096(4)
T4	$\mathbf{T_1}$	0.67(1) Fe, Zn + 0.33 Mg	1/3	–1/3	–0.1736(1)	0.0053(8)
M5	$\mathbf{T_1}$	0.50 Ti + 0.45(1) Fe, Zn + 0.05 Mg	–1/3	–2/3	–0.21608(8)	0.0073(5)
M6	**O**	1 Al	0.1646(2)	0.3291(3)	–0.29653(6)	0.0059(4)
T7	$\mathbf{T_2}$	0.43(1) Fe, Zn + 0.57 Mg	–1/3	–2/3	0.37083(8)	0.0071(6)
M8	$\mathbf{T_2}$	1 Al	–1/3	–2/3	0.3992(2)	0.0080(7)
T9	$\mathbf{T_2}$	0.57(1) Fe, Zn + 0.43 Mg	0	0	0.42401(5)	0.0082(5)
M10	**O**	1 Al	0	1/2	1/2	0.0079(4)
O1			–0.2965(7)	–0.1483(4)	–0.0535(1)	0.0089(8)
O2			–1/3	–2/3	–0.0587(3)	0.011(2)
O3			0.5114(4)	–0.5114(4)	–0.1488(1)	0.0122(8)
O4			0	0	0.1443(2)	0.011(1)
O5			–0.1642(4)	0.1642(4)	–0.2541(2)	0.0097(8)
O6			1/3	–1/3	–0.2538(3)	0.014(2)
O7			0.4809(4)	–0.4809(4)	–0.3472(1)	0.0104(9)
O8			0	0	–0.3392(2)	0.009(1)
O9			–0.1858(4)	0.1858(4)	0.4529(1)	0.0093(8)
O10			1/3	–1/3	0.4557(3)	0.007(2)
H			0	0	0.181(2)	0.08

Notes: Fe and Zn were refined with the scattering curve of Fe. The formula refined from X-ray analyses is $Al_{18.0}(Fe, Zn)_{5.1}Mg_{3.9}Ti_{1.0}O_{38}(OH)_2$.

TABLE 8. Modeled atomic coordinates of högbomite-12*H*, space group $P6_3mc$

Atom		Cation*	*x*	*y*	*z*
T1	$\mathbf{T_2}$	Mg, Fe	0	0	0.0208
M2	$\mathbf{T_2}$	Al	2/3	1/3	0.0417
T3	$\mathbf{T_2}$	Mg, Fe	1/3	2/3	0.0625
M4	**O**	Al	5/6	2/3	0.125
T5	$\mathbf{T_2}$	Mg, Fe	1/3	2/3	0.1875
M6	$\mathbf{T_2}$	Al	0	0	0.2083
T7	$\mathbf{T_2}$	Mg, Fe	2/3	1/3	0.2292
M8	**O**	Al	1/6	5/6	0.2917
M9	$\mathbf{T_1}$	Ti, Fe	1/3	2/3	0.375
T10	$\mathbf{T_1}$	Al	0	0	0.3958
M11	**O**	Al	5/6	2/3	0.4583
O1			1/3	1/6	0
O2			1/3	2/3	0
O3			0	0	0.0833
O4			0	1/2	0.0833
O5			2/3	1/3	0.1667
O6			2/3	5/6	0.1667
O7			1/3	1/6	0.25
O8			1/3	2/3	0.25
O9			0	0	0.3333
O10			0	1/2	0.3333
O11			2/3	1/3	0.4167
O12			2/3	5/6	0.4167
H			2/3	1/3	0.38

* Assumed composition.

stacking sequence of the oxygen layers, ABACBACABCBACB ABCACBACBC or *chccchcc hccchcchccchc* (Table 10), is the same as found for nigerite-24*R* (Grey and Gatehouse 1979).

The average octahedral Al-O distances vary between 1.909 and 1.946 Å where the longest distance is found within the nolanite-like module for the **O**-layer (bearing M1) separating two $\mathbf{T_1}$-layers. Mg with minor Fe yielding T-O distances between 1.915 and 1.956 Å occupies the tetrahedral positions of the $\mathbf{T_2}$-layer. The T3 site in the $\mathbf{T_1}$-layer has an average T3-O distance of 1.848 Å. Site-population refinement indicates that this site is 83% occupied by Mg and/or Al with the remaining 17% being Fe. However, the T3-O distance is too long for Al (expected value 1.73 Å, Brown 1996) and too short for Mg (expected value 1.95 Å, Brown 1996). Thus a mixed Mg/Al occupation must be assumed, which explains why the T3-O distance is 0.1 Å shorter than the T6-O distance. T6 is occupied by 83% Mg and 17% Fe (Table 6). The average chemical analysis yields ca. 42 Al pfu (Table 4). However, the formula provides 48 M sites pfu of which six are occupied by Ti and Fe, leaving 42 Al on octahedrally coordinated sites. If Al partly occupies the T3 site some octahedral Al must be replaced by

TABLE 9. Modeled atomic coordinates of högbomite-14*T*, space group $P\bar{3}m1$

Atom		Cation*	*x*	*y*	*z*
M1	$\mathbf{T}_2$	Al	0	0	0
T2	$\mathbf{T}_2$	Mg, Fe	2/3	1/3	0.0179
M3	**O**	Al	2/3	5/6	0.0714
T4	$\mathbf{T}_2$	Mg, Fe	2/3	1/3	0.125
M5	$\mathbf{T}_2$	Al	1/3	2/3	0.1429
T6	$\mathbf{T}_2$	Mg, Fe	0	0	0.1607
M7	**O**	Al	1/2	0	0.2143
M8	$\mathbf{T}_1$	Ti, Fe	0	0	0.2857
T9	$\mathbf{T}_1$	Al	1/3	2/3	0.3036
M10	**O**	Al	5/6	2/3	0.3571
T11	$\mathbf{T}_2$	Mg, Fe	1/3	2/3	0.4107
M12	$\mathbf{T}_2$	Al	2/3	1/3	0.4286
T13	$\mathbf{T}_2$	Mg, Fe	0	0	0.4464
M14	**O**	Al	0	1/2	1/2
O1			1/3	1/6	0.0357
O2			1/3	2/3	0.0357
O3			1/2	0	0.1071
O4			0	0	0.1071
O5			2/3	5/6	0.1786
O6			2/3	1/3	0.1786
O7			5/6	2/3	0.25
O8			1/3	2/3	0.25
O9			2/3	5/6	0.3214
O10			2/3	1/3	0.3214
O11			1/2	0	0.3929
O12			0	0	0.3929
O13			1/3	1/6	0.4643
O14			1/3	2/3	0.4643
H			2/3	1/3	0.29

* Assumed composition.

TABLE 10. Schematic representation of cation and oxygen stacking in högbomite-24*R*, nomenclature explained in the text

Oxygen stacking		Oxygen atom	Type of layer	Cation	
				$T^{[4]}$	$M^{[6]}$
C	*c*	O1, O2			
			$\mathbf{T}_1$	T3, H	M2
B	*h*	O3, O4			
			O		M4
C	*c*	O5, O6			
			$\mathbf{T}_2$	T6, T7	M5
A	*c*	O7, O8			
			O		M8
B	*c*	O7, O8			
			$\mathbf{T}_2$	T6, T7	M5
C	*c*	O5, O6			
			O		M4
A	*h*	O3, O4			
			$\mathbf{T}_1$	T3, H	M2
C	*c*	O1, O2			
			O		M1
B	*c*	O1, O2			
			$\mathbf{T}_1$	T3, H	M2
A	*h*	O3, O4			
			O		M4
B	*c*	O5, O6			
			$\mathbf{T}_2$	T6, T7	M5
C	*c*	O7, O8			
			O		M8
A	*c*	O7, O8			
			$\mathbf{T}_2$	T6, T7	M5
B	*c*	O5, O6			
			O		M4
C	*h*	O3, O4			
			$\mathbf{T}_1$	T3, H	M2
B	*c*	O1, O2			
			O		M1
A	*c*	O1, O2			
			$\mathbf{T}_1$	T3, H	M2
C	*h*	O3, O4			
			O		M4
A	*c*	O5, O6			
			$\mathbf{T}_2$	T6, T7	M5
B	*c*	O7, O8			
			O		M8
C	*c*	O7, O8			
			$\mathbf{T}_2$	T6, T7	M5
A	*c*	O5, O6			
			O		M4
B	*h*	O3, O4			
			$\mathbf{T}_1$	T3, H	M2
A	*c*	O1, O2			
			O		M1 (origin)

TABLE 11. Schematic representation of cation and oxygen stacking in högbomite-10*T*, nomenclature explained in the text

Oxygen stacking		Oxygen atom	Type of layer	Cation	
				$T^{[4]}$	$M^{[6]}$
A	*c*	O1, O2			
			O		M3
C	*c*	O3, O4			
			$\mathbf{T}_1$	T4	M5
B	*h*	O5, O6			
			O		M6
C	*c*	O7, O8			
			$\mathbf{T}_2$	T7, T9	M8
A	*c*	O9, O10			
			O		M10
B	*c*	O9, O10			
			$\mathbf{T}_2$	T7, T9	M8
C	*c*	O7, O8			
			O		M6
A	*h*	O5, O6			
			$\mathbf{T}_1$	T4	M5
C	*c*	O3, O4			
			O		M3
B	*c*	O1, O2			
			$\mathbf{T}_2$	T2	M1 (origin)
A	*c*	O1, O2			
			O		M3

Mg that has a similar scattering power for X-rays. The most probable candidate for partial Mg incorporation is the M1 site that has the longest average M1-O distance of 1.947 Å.

There is no doubt that M2 is the Ti-bearing site because the scattering power of all other octahedrally coordinated positions is characteristic of Al and/or Mg (Table 6). Based on the analyzed Ti concentration the octahedral position (M2) of the $\mathbf{T}_1$-layer was constrained to have 4.7 Ti pfu (78% Ti) and the remaining 22% refined to Fe and Mg yielding an average M2-O distance of 2.021 Å. The M2 octahedron bonds to 3 × O1 in one oxygen layer and 3 × O3 in an other oxygen layer. O3 is only threefold-coordinated by cations (1 × M2, and 2 × M4) whereas O1 is fourfold-coordinated (2 × M1, 1 × M2, and 1 × T3). This non-uniform oxygen environment around M2 leads to an out-of-center distortion of the M2 cations where M2-O3 distances are 1.882 Å and M2-O1 distances are 2.165 Å. In particular Ti^{4+} is suited to adopt such distortions that can be understood on the basis of the second-order Jahn-Teller theorem characteristic of d^0 transition metal cations (Kunz and Brown 1995). In nigerite-24*R* where corresponding coordinations were found (Grey and Gatehouse 1979) the M2 position is completely occupied by Sn^{4+} that is not a d^0 cation and thus the distortion is less pronounced with 3 × Sn-O3 of 2.003 Å and 3 × Sn-O1 of 2.108 Å.

Högbomite-10*T*. This polysome is formed by alternation of nolanite-like and spinel modules in the sequence *NSSNS* leading to the general formula $T_8M_{20}O_{38}(OH)_2$. The stacking sequence of the oxygen layers is ABCACBACBC or *ccchccccchc* (Table 11).

The M sites (M3, M6, M10) of all **O**-layers and the octahe-

TABLE 12. Schematic representation of cation and oxygen stacking in högbomite-12*H*, nomenclature explained in the text

Oxygen stacking	Oxygen atom	Type of layer	Cation T[4]	 M[6]
A *c*	O1, O2			
		O		(origin) M11
C *h*	O11, O12			
		$\mathbf{T}_1$	T10	M9
A *c*	O9, O10			
		O		M8
B *c*	O7, O8			
		$\mathbf{T}_2$	T5, T6	M6
C *c*	O5, O6			
		O		M4
A *c*	O3, O4			
		$\mathbf{T}_2$	T1, T3	M2
B *c*	O1, O14			
		O		M11
C *h*	O11, O12			
		$\mathbf{T}_1$	T10	M9
B *c*	O9, O10			
		O		M8
A *c*	O7, O8			
		$\mathbf{T}_2$	T5, T7	M6
C *c*	O5, O6			
		O		M4
B *c*	O3, O4			
		$\mathbf{T}_2$	T1, T3	M2
A *c*	O1, O2			
		O		(origin) M11

TABLE 13. Schematic representation of cation and oxygen stacking of högbomite-14*T*, nomenclature explained in the text

Oxygen stacking	Oxygen atom	Type of layer	Cation T[4]	 M[6]
A *c*	O1, O2			
		$\mathbf{T}_2$	T1	M2 (origin)
B *c*	O1, O2			
		O	M3	
C *c*	O3, O4			
		$\mathbf{T}_2$	T4, T6	M5
B *c*	O5, O6			
		O	M7	
A *h*	O7, O8			
		$\mathbf{T}_1$	T9	M8
B *c*	O8, O9			
		O	M10	
C *c*	O11, O12			
		$\mathbf{T}_2$	T11, T13	M12
A *c*	O13, O14			
		O	M14	
B *c*	O13, O14			
		$\mathbf{T}_2$	T11, T13	M12
C *c*	O11, O12			
		O	M10	
A *c*	O9, O10			
		$\mathbf{T}_1$	T9	M8
B *h*	O7, O8			
		O	M7	
A *c*	O5, O6			
		$\mathbf{T}_2$	T4, T6	M5
C *c*	O3, O4			
		O	M3	
B *c*	O1, O2			
		$\mathbf{T}_2$	T1	M2 (origin)
A *c*	O1, O2			
		O	M3	

TABLE 14. Selected interatomic distances (Å) for högbomite-24*R*

M1	O2	2×	1.933(1)	M5	O5	3×	1.899(2)
	O1	4×	1.952(1)		O7	3×	1.919(2)
average			1.946	average			1.909
M2	O3	3×	1.882(2)	T6	O6	1×	1.954(3)
	O1	3×	2.165(2)		O7	3×	1.957(2)
	average		2.024	average			1.956
T3	O4	1×	1.847(3)	T7	O5	3×	1.906(2)
	O1	3×	1.848(2)		O8	1×	1.941(3)
	average		1.848	average			1.915
M4	O6	1×	1.906(2)	M8	O7	4×	1.904(1)
	O3	2×	1.920(1)		O8	2×	1.951(1)
	O4	1×	1.935(2)	average			1.920
	O5	2×	1.971(1)				
	average		1.937				

TABLE 15. Selected interatomic distances (Å) for högbomite-10*T*

M1	O1	6×	1.915(3)	M6	O5	2×	1.896(2)
average			1.915		O8	1×	1.902(3)
					O6	1×	1.938(3)
T2	O1	3×	1.940(4)		O7	2×	1.960(2)
	O2	1×	1.940(7)	average			1.925
average			1.940				
				T7	O7	3×	1.917(4)
M3	O2	1×	1.896(4)		O10	1×	1.951(6)
	O1	2×	1.924(3)	average			1.926
	O3	2×	1.925(2)				
	O4	1×	1.944(3)	M8	O7	3×	1.887(4)
average			1.923		O9	3×	1.912(4)
				average			1.900
T4	O6	1×	1.846(6)				
	O3	3×	1.852(4)	T9	O8	1×	1.950(5)
average			1.851		O9	3×	1.956(4)
				average			1.955
M5	O5	3×	1.889(4)				
	O3	3×	2.180(4)	M10	O9	4×	1.902(2)
average			2.035		O10	2×	1.939(3)
				average			1.914

drally coordinated sites (M1, M8) of the $\mathbf{T}_2$-layer revealed low electron densities characteristic of Al. Corresponding mean octahedral Al-O distances are between 1.900 and 1.925 Å. Only the M5 site displayed a mean density of ca. 23 electrons characteristic of transition metals. According to electron-microprobe analyses the occupation of the octahedral position (M5) in the $\mathbf{T}_1$-layer was fixed at 50% Ti. The remaining 50% of the M5 position converged to 45% Fe and 5% Mg. As already discussed for the 24*R* polysome, the Ti-bearing site has a non-uniform oxygen coordination. M5 bonds 3× to O3 within 2.180 Å and 3× to O5 within 1.889 Å. O3 in one oxygen layer is fourfold-coordinated by cations whereas O5 in the adjacent oxygen layer is threefold-coordinated. Thus the Ti^{4+} out-of-center distortion benefits from the second-order Jahn-Teller theorem for d^0 cations (Kunz and Brown 1995). The T4 site that shares the $\mathbf{T}_1$-layer with M5 has an average T4-O distance of 1.851 Å. Site-occupancy refinements led to 0.67 (Fe, Zn) and 0.33 (Mg, Al). As for the corresponding tetrahedron in högbomite-24*R*, the rather short T4-O distance (1.851 Å) suggests that the T4 site is to approximately equal amounts occupied by large divalent (Fe, Mg, Zn) and small trivalent (Fe, Al) cations. Other average T-O distances varied between 1.926 and 1.955 Å. The refined formula $Al_{18}Mg_{3.9}(Zn,Fe)_{5.1}Ti_1O_{38}(OH)_2$ is in good agreement with

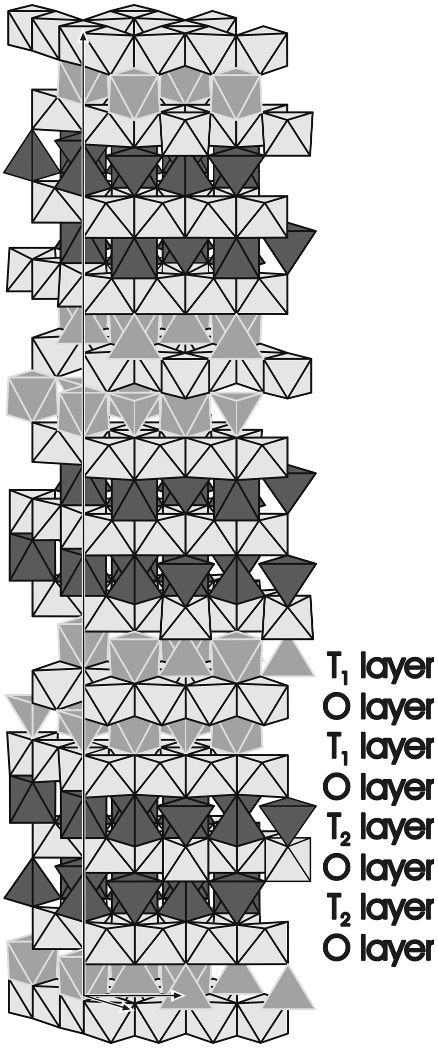

FIGURE 2. The polyhedral stacking sequence in högbomite-24*R* is $3\times$(**T$_1$-O-T$_1$.O-T$_2$-O-T$_2$-O**).

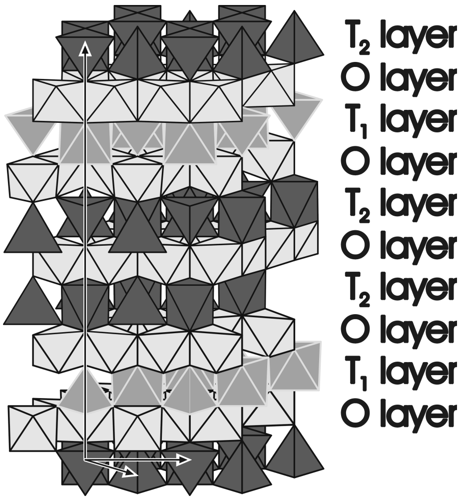

FIGURE 3. The polyhedral stacking sequence in högbomite-10*T* is **T$_1$-O-T$_2$-O-T$_2$-O-T$_1$-O-T$_2$-O**.

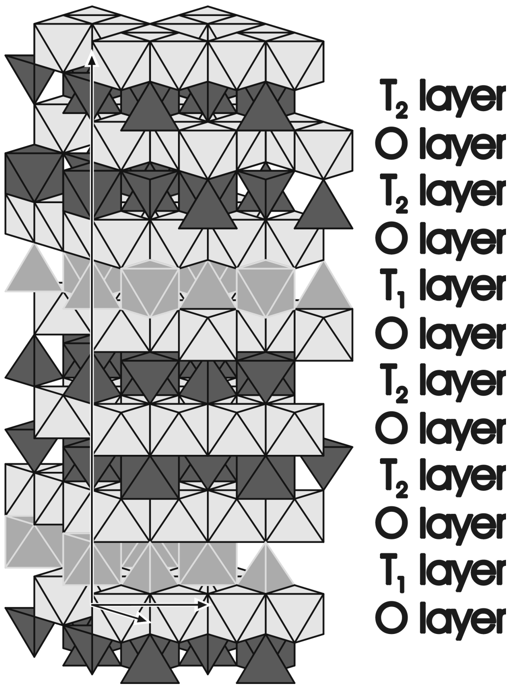

FIGURE 4. The polyhedral stacking sequence in högbomite-12*H* is **T$_1$-O-T$_2$-O-T$_2$-O-T$_1$-O-T$_2$-O-T$_2$-O**.

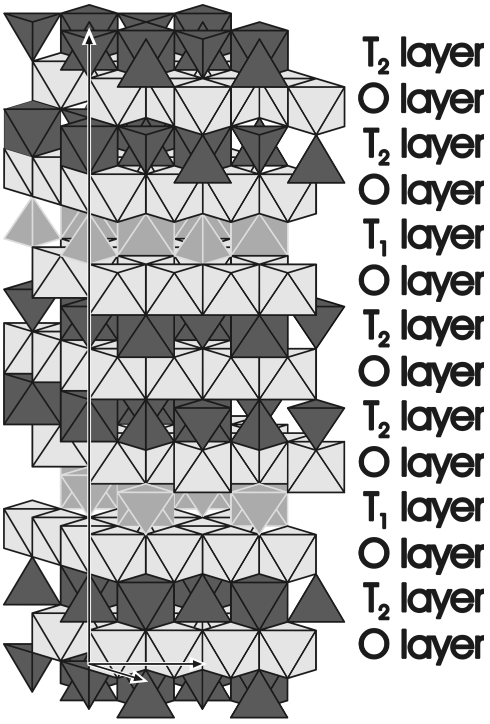

FIGURE 5. The polyhedral stacking sequence in högbomite-14*T* is **T$_1$-O-T$_2$-O-T$_2$-O-T$_1$-O-T$_2$-O-T$_2$-O-T$_2$-O**.

the composition $Al_{18.29}Mg_{3.77}(Fe,Zn,Mn, Ni)_{4.94}Ti_{1.00}O_{38}(OH)_2$ calculated from electron microprobe analyses performed on the same crystal. Notice that the electron-microprobe analyses only served to determine the type of cations (for assignment of scattering curves) and to constrain the Ti concentration in the structure refinement. Thus the good agreement between refined occupancies and analyzed composition confirms the structural model.

DISCUSSION

Do the Ti^{4+} and Sn^{4+} contents determine the type of polysome?

Based on the stacking periodicity along the **c**-axis, determined by single-crystal X-ray methods, McKie (1963) identified högbomites with a 10-layer repeat sequence from an emery deposit in North Carolina (Friedman 1952), from eastern Transvaal (Nel 1949), and from skarns in Tanganyika (McKie 1963). McKie (1963) also presented an X-ray powder diffraction pattern for a polysome with a 10-layer repeat sequence, to which Zakrzewski (1977), Beukes et al. (1986), and Grew et al. (1987) referred when identifying their högbomite polysomes. Chemical compositions of högbomite-10*T* that have been reported so far do not show a unique pattern. The Ti concentration, expressed in apfu based on 28 cations, ranges from 1.66 for högbomite-10*T* from Mg-rich skarns at Mautia Hill, Tanganyika (McKie 1963), and 1.65 Ti pfu for a sample from Letaba district, Transvaal (Nel 1949), to 1.0 Ti pfu for högbomite from Corundum Creek (South Australia), and 0.73–1.12 for högbomite-10*T* from a cordierite-gedrite-phlogopite schist in Bushmanland, South Africa (Beukes et al. 1986). Provided that the polysome identification based on a few X-ray powder lines is correct for a högbomite-10*T* from a kornerupine-cordierite-sillimanite rock from Tamil Nadu, India (Grew et al. 1987), this sample has only 0.50 Ti pfu (0.018 Ti per one cation).

Only one other högbomite with a 24-layer repeat sequence has been described, as lamellar inclusions within gem quality spinels from Tanzania (Schmetzer and Berger 1990). This högbomite is essentially Fe-free and has high Ti concentrations. If the formula is normalized to 66 cations ca. 6.3 Ti pfu result (0.095 Ti per one cation) that is significantly higher than the 4.7 Ti pfu determined for the högbomite-24*R* from Liganga studied in this paper. Although only two samples of högbomite-24*R* have been crystallographically and chemically analyzed, it is striking that both samples have about twice the Ti concentration of the more common högbomite-8*H* polysomes with the same ratio of *N* and *S* modules. Thus it may be assumed that the Ti^{4+} content determines the type of polysome formed.

There is a striking difference in the polysomatic behavior of nigerites (Sn-rich) and högbomites (Ti-rich). 6*T* and 24*R* are the major polysomes occurring in nigerites developed as crystals. Neiva and Champness (1997) also reported isolated domains of other polysomes (e.g., 30*R*, 18*R*) observed by HRTEM. The 6*T* and 24*R* polysomes are similar in that (1) two nolanite-like modules are adjacent to each other, (2) the **O**-layer separating two $\mathbf{T_1}$ sheets contains hydroxyl on both sites (Fig. 6), (3) all structure studies report significant amounts (25–33 %) of octahedral vacancies in this latter **O**-layer, and (4) the octahedrally coordinated site in the $\mathbf{T_1}$-layer shows only a weak out-of-center distortion. Very Sn-rich nigerites crystallize with the structure of the 6*T* polysome whereas nigerites with less Sn prefer the 24*R* polysome (e.g., Neiva and Champness 1997). This polysome selectivity is caused by the different ratio of spinel and nolanite-like modules in these polysomes (0.5 for nigerite-6*T* and 1.0 for nigerite-24*R*) whereas only the nolanite module incorporates Sn^{4+}. As a rule of thumb for nigerites, the octahedrally coordinated M site in the $\mathbf{T_1}$-layer is completely occupied by Sn. There are also nigerites belonging to polysomes that are considerably richer in spinel modules (e.g., Schumacher et al. 1987; Petersen et al. 1989). However, these nigerite-group minerals have Ti^{4+} combined with decreased Sn^{4+} and behave similar to högbomites (the M site in the $\mathbf{T_1}$-layer is only partially occupied by Ti^{4+} and Sn^{4+}).

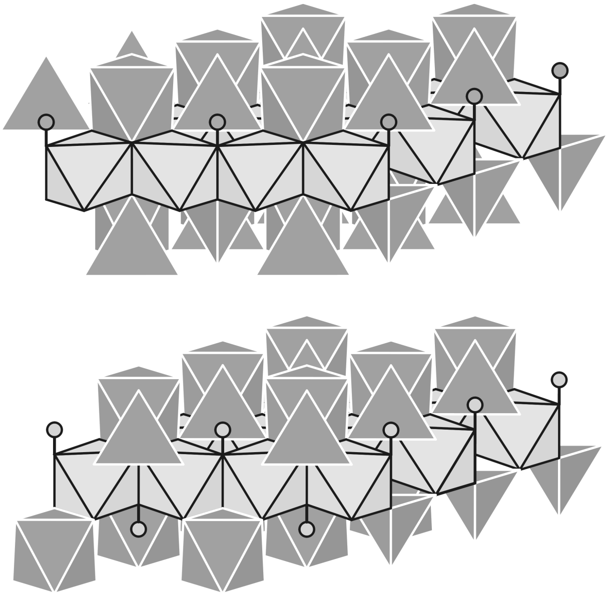

FIGURE 6. **O**-layer in nolanite (Gatehouse et al. 1983) with hydroxyl groups attached on one side (top) and **O**-layer of the nolanite module in högbomite-24*R* (this study), nigerite-6*T* (Arakcheeva et al. 1995), and nigerite-24*R* (Grey and Gatehouse 1979) with hydroxyl groups attached on both sides (bottom).

For högbomite-group minerals the 8*H* and the 10*T* polysomes dominate (McKie 1963; Petersen et al. 1989). The 6*T* polysome has not yet been described and the 24*R* polysome is very rare. Notice that the 6*H* polysomes described by McKie (1963) and Petersen et al. (1989) are actually 12*H* polysomes according to the nomenclature of Peacor (1967) (used in this paper). Högbomite 8*H* and 10*T* polysomes are similar in that (1) isolated nolanite-like modules are always sandwiched by spinel modules, (2) an **O**-layer adjacent to a $\mathbf{T_1}$ sheets contains hydroxyl on only one side (Fig. 6), (3) there are no vacancies in the latter **O**-layer, and (4) the octahedrally coordinated site in the $\mathbf{T_1}$-layer shows a strong out-of-center distortion. There seems to be no correlation between Ti content and type of polysome. The octahedrally coordinated M site in the $\mathbf{T_1}$-layer is most frequently half-occupied by Ti with additional Fe. The only exception is högbomite-24*R* as discussed above.

The Ti^{4+} and Sn^{4+} substitution mechanism in högbomite and nigerite

We assume that each module itself is approximately charge-balanced, as suggested by the available structure refinements (Grey and Gatehouse 1979; Gatehouse and Grey 1982; Chen et al. 1989; Arakcheeva et al. 1995; Armbruster 1998; Armbruster et al. 1998). This implies that variable Ti^{4+} and/or Sn^{4+} incorporation is charge balanced in the nolanite unit, $TM_4O_7(OH)$. As a starting model we assume that a nolanite-like module is composed of only trivalent cations. Thus incorporation of Ti^{4+} or Sn^{4+} follows in the most simple case the equation (Ti^{4+}, Sn^{4+}) + (Mg, Fe^{2+}, Zn) $\leftrightarrow$ 2 (Al, Fe^{3+}) and the question arises as to which sites are involved. All structural studies (Grey and Gatehouse 1979; Gatehouse and Grey 1982; Chen et al. 1989; Arakcheeva et al. 1995; Armbruster 1998; this paper) except one (Armbruster et al. 1998) assign the four-valent cations to the octahedrally coordinated (M) site in the $\mathbf{T_1}$-layer. Independently of whether the octahedron is partly or fully occupied by Ti^{4+} or Sn^{4+} the mean M-O distances of this site vary (according to the above structure refinements) between 2.021 and 2.056 Å. The tetrahedron in the same $\mathbf{T_1}$-layer has mean T-O distances between 1.834 and 1.878. These rather constant values probably arise because the $\mathbf{T_1}$-layer in these structures is sandwiched between two **O**-layers occupied mainly by Al. In the case of högbomite-group minerals, where the M site in the $\mathbf{T_1}$-layers is approximately half-occupied by Ti^{4+}, charge balance may be achieved by Fe^{2+} in the same site. According to Brown (1996) the mean octahedral Fe^{2+}-O distance is 2.141 Å and the corresponding Ti^{4+}-O distance is 1.965 Å, yielding an average distance of 2.053 Å, which is close to the value observed in högbomite-group minerals. In addition, this site may also host Fe^{3+}, which has a characteristic Fe^{3+}-O distance of 2.015 Å (Brown 1996). This means that the relevance of the T site in the $\mathbf{T_1}$-layer for charge balance depends on the Ti^{4+} and Fe^{2+} concentration in the octahedron.

Armbruster et al. (1998) assigned Ti^{4+} in zincohögbomite-16*H* to the **O**-layer in the nolanite-like module. However, based on improved knowledge due to the additional structure refinements performed in this study, this assignment may be questioned. The complex composition of this högbomite, comprising Zn, Ti, and Fe, does not allow for a definite assignment for Ti. The out-of-center distortion of the octahedrally coordinated site (M8) in the $\mathbf{T_1}$-layer is similar to other högbomite polysomes. Thus Ti^{4+} may prefer this asymmetric site (Kunz and Brown 1995). The increased T1-O distance (1.922 Å) for the tetrahedron in the $\mathbf{T_1}$-layer suggests that Ti^{4+} charge balance is mainly achieved in this polysome by tetrahedrally coordinated Zn incorporation.

The substitution mechanism is different for nigerites (6*T* and 24*R*) where the M site in the $\mathbf{T_1}$-layer is almost completely occupied by Sn^{4+}. The rigid size of the T site (in $\mathbf{T_1}$) excludes incorporation of high concentrations of Fe^{2+}, Zn^{2+}, and Mg^{2+} for charge balance. Both of the two known nigerite polysomes (24*R* and 6*T*) have adjacent nolanite modules (Grey and Gatehouse 1979; Arakcheeva et al. 1995) and the excess charge (due to Sn^{4+} incorporation) is neutralized in the **O**-layer between two $\mathbf{T_1}$-layers. The electron density in this **O**-layer is lower than expected for octahedrally coordinated Al, which supports this argument. Thus, in structure refinements of nigerite-group minerals (Grey and Gatehouse 1979; Chen et al. 1989; Arakcheeva et al. 1995) between 25 and 30% octahedral vacancies were refined. The exchange equation can be written as $3Sn^{4+}$ + vacancy $\leftrightarrow$ 4 (Al, Fe^{3+}). The octahedral site in the **O**-layer has three times the multiplicity of the octahedral site in the $\mathbf{T_1}$-layer. Thus, 22% vacancies would be expected in the intercalated **O**-layer if two adjacent $\mathbf{T_1}$-layers have the octahedra completely occupied by Sn^{4+}.

Armbruster (1998) has argued that charge balance in nigerites could also be achieved by Li instead of vacancies: 2 Sn^{4+} + Li^{+} $\leftrightarrow$ 3 (Al, Fe^{3+}). Lithium has not yet been analyzed in nigerites but the close geochemical association of Li and Sn in pegmatites would support such a substitution. Both vacancies and octahedrally coordinated Li would lead to an expansion of the dominantly Al occupied octahedra. Arakcheeva et al. (1995) observed an M-O distance of 1.961 Å for the low-electron density M site in nigerite-6*T*, and Grey and Gatehouse (1979) measured 1.957 Å for the corresponding site in nigerite-24*R*. M-O distances in completely Al occupied octahedral sites vary between 1.89 and 1.92 Å in these structures.

The Ti^{4+} charge-balancing mechanism in högbomite-24*R* (this study), where the octahedron in the $\mathbf{T_1}$-layer is 78% occupied by Ti^{4+} and reduced electron density could not be found in the intercalated **O**-layer is of interest. Assuming that 0.17 Fe^{2+} and 0.05 Mg complete the occupancy of the octahedron, a mean M-O distance of 2.00 Å can be expected (Brown 1996) which is in good agreement with the observed value of 2.02 Å. The tetrahedrally coordinated site in the $\mathbf{T_1}$-layer is too small to host the remaining 0.64 divalent cations for charge balance. However, it is striking that two **O**-layers adjacent to the $\mathbf{T_1}$-layers reveal increased M-O distances of 1.947 Å (M1) and 1.937 Å (M4). If Ti^{4+} charge balance operates according to 1 Ti^{4+} + 1 Mg^{2+} $\leftrightarrow$ 2 (Al, Fe^{3+}), each M site in these **O**-layers would be occupied by 0.64/3 = 21% Mg (division by 3 becomes necessary due to the 3× higher multiplicity of the M site in the **O**-layer). This model leads to a mean M-O distance of ~1.95 Å, which is slightly higher than the observed value. This discrepancy could be explained by the additional charge-balancing influence of the tetrahedron (T3) in the $\mathbf{T_1}$-layer.

Hydroxyl ion in högbomite and nigerite

Previous studies questioned whether högbomites and nigerites are hydrous minerals (for a review on this subject see Schumacher et al. 1987). The most recent structure refinements on nigerite-6*T* (Arakcheeva et al. 1995), zincohögbomite-8*H* (Armbruster 1998), högbomite-24*R* (this study), and högbomite-10*T* (this study) have located and refined a hydrogen position associated with each nolanite module. Furthermore, bond-valence calculations clearly disclose an OH-group and also a hydrogen-bond acceptor.

In högbomite-24*R* O2 and O3 are threefold-coordinated by cations whereas all other oxygen atoms are fourfold-coordinated. O2 and O3 are under-saturated and have low bond-valence sums, 1.40 and 1.77 v.u., respectively. A table of bond-valence calculations (Brown 1996) of all atoms is deposited as Appendix 3. Because O2 has the lowest bond-valence sum it is expected to be an OH site. The H atom was successfully located ca. 0.8 Å from the O2 atom on the threefold axis. The under-saturated O3 atom located at a distance of 2.35 Å to the H atom acts as hydrogen-bond acceptor. The three O3 atoms form a triangle centered by a threefold axis. As pointed out by Armbruster (1998) it is more likely for the H atom to occupy a position on one O2-O3 vector rather than directly above the O2 atom, which would lead to a trifurcated hydrogen bond. An H position displaced from the threefold axis can only be one-third occupied. A section of the difference-Fourier map perpendicular to the **c**-axis at the height of the hydrogen position shows a triangular distribution of positive electron density. This supports the assumption of three H positions each being one-third occupied by.

According to the bond-valence sums of the atoms in högbomite-10*T* (Appendix 4) O4 (1.36 v.u.) is an OH group and O5 (1.78 v.u.) is the acceptor of the hydrogen bond. The H atom was successfully located ca. 0.8 Å from the O4 atom on the threefold axis. Similar to högbomite-24*R* the difference-Fourier peak assigned to the H atom has a triangular form in sections perpendicular to the **c**-axis.

In högbomite-10*T* and högbomite-24*R* the H atoms point towards the tetrahedral vacancies of the $\mathbf{T}_1$-layers. In högbomite-24*R* OH groups are attached to both sites of the **O**-layer (bearing M1) that is sandwiched between two $\mathbf{T}_1$-layers (Fig. 6). Such layers that contain hydroxyl on both sides do not occur in högbomite-10*T*, the nolanite structure, or in other hitherto refined högbomite or zincohögbomite polysomes (8*H*, 16*H*). **O**-layers with hydroxyl on both sides also exist in nigerite-24*R* (Grey and Gatehouse 1979) and in nigerite-6*T* (Arakcheeva et al. 1995).

An FTIR spectrum (Fig. 7) of a högbomite-10*T* single-crystal shows an absorption at 3350 cm^{-1} that can be interpreted as an O-H stretching band, although it is a rather weak signal for stoichiometric OH. Thus there is no doubt that högbomites and nigerites are hydrous minerals.

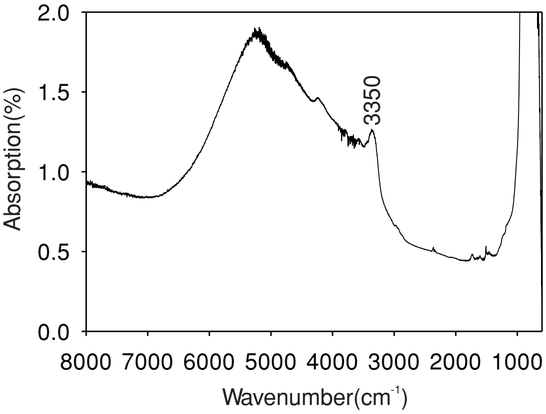

FIGURE 7. FTIR spectrum of a single-crystal of högbomite-10*T*.

COMPARISON WITH OTHER *S*-MODULE BEARING POLYSOMATIC SERIES

The system of magnetoplumbite-related structures is comparable to the polysomatic series of högbomite- and nigerite-group minerals. In addition to magnetoplumbite (e.g., Moore et al. 1989; Bermanec and Šćavničar 1993) and related minerals (e.g., hawthornite: Haggerty et al. 1989; haggertyite: Grey et al. 1998; nežilovite: Bermanec et al. 1996; batiferrite: Lengauer et al. 2001), several synthetic hexagonal ferrites and hexagonal aluminates have been intensively investigated because of their technical applications as ferrimagnetics (hexaferrite) and solid-state electrolytes (hexa-aluminates) (e.g., Kummer 1972; Iyi et al. 1989; Kojima 1982).

The similarity between the polysomatic series of högbomites and magnetoplumbite-related structures is manifold: (1) Both exhibit cubic and hexagonal closest-packing of oxygen layers, (2) both are composed of two or more modules, (3) of which one is the spinel module. (4) The different modules can be stacked in various ratios. (5) Both structure types have comparable lattice parameters.

Magnetoplumbite-related compounds are characterized by cubic (*c*) and hexagonal (*h*) closest-packed oxygen layers parallel to (001). A sequence of two cubic closest-packed layers represents the spinel module (or *S*-block) with small cations (Y) distributed in octahedrally and tetrahedrally coordinated sites. A sequence of three hexagonal closest-packed layers is referred to as conductor layer (Iyi et al. 1989) or *R*-block (Kohn and Eckart 1964). The central of the three hexagonal closest-packed oxygen layers has three instead of four oxygen atoms, because one is replaced by a large cation (A). Furthermore, the *R*-block hosts cations (Y) that are situated in octahedrally coordinated sites between the oxygen layers and in-between three oxygen atoms of the central oxygen layer, resulting in a trigonal-bipyramidal coordination. The composition of the *R*-block is AY_6O_{11}. The spinel module (*S*-block) and the conductor layer (*R*-block) can be stacked in different ratios. For magnetoplumbite *S*- and *R*-blocks alternate, hence the formula for *RS* is $AY_6O_{11}{\cdot}Y_6O_8 = AY_{12}O_{19}$. In magnetoplumbite-related structures the length of **a** is similar to that in the högbomite series (~5.6 Å). The length of **c** depends on the stacking sequence.

The Mg-free Ca-hexaaluminate $CaAl_{12}O_{19}$ has the magnetoplumbite-type structure (Kato and Saalfeld 1968) and is found in nature as the mineral hibonite (Curien et al. 1956; Bermanec et al. 1996). One of the most important differences between the spinel modules in högbomite- and nigerite-group minerals on one hand and hexaaluminate-related compounds on the other is the charge of the module. As shown above högbomite- and nigerite-group minerals have approximately uncharged spinel and nolanite modules. However, the *R* module in hexa-aluminates, e.g., in hibonite, is anionic $[CaAl_6O_{11}]^{2-}$. To be balanced it requires a cationic spinel module composed of $[Al_6O_8]^{2+}$. More complex polysomes in this group of compounds (Göbbels et al. 1995; Iyi et al. 1995) can only be obtained by introduction of additional neutral spinel modules (e.g., of composition $Mg_2Al_4O_8$). In the system CaO-MgO-Al_2O_3 the polysomatic structures CAM I and CAM II (Iyi et al. 1995) were described. CAM I, $Ca_2Mg_2Al_{28}O_{46}$, $a = 5.573$, $c = 79.810$ Å, $R\overline{3}m$, $Z = 3$, has the stacking sequence *RSRSS*, $2(AY_6O_{11}){\cdot}3(Y_6O_8) = A_2Y_{18}O_{27}$, and CAM II, $CaMg_2Al_{16}O_{27}$, $a = 5.590$, $c = 31.288$ Å, $P\overline{6}m2$, $Z = 2$, has the stacking sequence *RSS*, $AY_6O_{11}{\cdot}2(Y_6O_8) = AY_{18}O_{27}$.

For hexaaluminates with Mg and Al as small Y-cations and Ba as the large A-cation two stable compounds are reported (Göbbels et al. 1998). These have a conductor layer of β-alumina type. The β-alumina-structure type is very similar to the magnetoplumbite-structure type, but in the conductor layer of the β-alumina structure the central of the three closest-packed oxygen layers contains only one oxygen atom and one large A cation. Small cations (Y) are situated in tetrahedrally coordinated sites between the oxygen layers of the conductor layer. Hence, the conductor layer of β-alumina type (AY_5O_9) is rather loose packed. BAM I (Iyi et al. 1986), $BaMgAl_{10}O_{17}$, $a = 5.628$, $c = 22.659$ Å, $P6_3/mmc$, $Z = 2$, has β-alumina structure with the stacking sequence $R_\beta S$, $AY_5O_9{\cdot}Y_6O_8 = AY_{11}O_{17}$. The structure of BAM II (Iyi et al. 1998) with a stacking sequence $R_\beta SS$, $AY_5O_9{\cdot}2(Y_6O_8) = AY_{17}O_{25}$, has composition $Ba_2Mg_6Al_{28}O_{50}$, $a = 5.638$, $c = 31.983$ Å, $P\bar{6}m2$, $Z = 2$.

On the symmetry of högbomite polysomes

It is worth noticing that for högbomite and related compounds only the space groups $P\bar{3}m1$, $R\bar{3}m$, and $P6_3mc$ have been found to date (Table 1). A similar phenomenon has been observed in other compounds derived from closest-packing of atoms. To give an example, for SiC polytypes the space groups $P3m1$, $R3m1$, and $P6_3mc$ are known (Patterson and Kasper 1959). In addition, the hexaaluminates discussed in the former chapter exhibit only space groups $R\bar{3}m$, $P6_3/mmc$, and $P\bar{6}m2$.

It is well known (e.g., Patterson and Kasper 1959; Verma and Krishna 1966) that a periodic stacking of closest-packed layers can exhibit $P3m1$, $R3m1$, $P\bar{3}m1$, $R\bar{3}m$, $P\bar{6}m2$, $P6_3mc$, $P6_3/mmc$, or $F\bar{4}3m$ symmetry. The symmetry of the closest-packed layers (e.g., anions) is lowered by intercalated atoms (e.g., cations) and by the physical chemistry of the system. The overall symmetry of the structure including all atoms is expected to be in a group-subgroup- relationship with the symmetry of the closest-packed assemblage alone. For an explanation of the observed space groups for högbomite two structural principles are of relevance:

(1) The anion packing is characterized by an even number of oxygen layers, which are stacked in cubic and hexagonal closest-packed fashion (Gatehouse and Grey 1982; Grey and Gatehouse 1979). The intercalation of a hexagonal closest-packed oxygen layer into a sequence of cubic closest-packed oxygen layers for högbomite and related compounds takes place in such a way that a mirror plane is introduced. All structures composed of closest-packed spheres containing horizontal symmetry planes have the same hexagonal symmetry $P6_3/mmc$ (Shubnikov and Koptsik 1974). In $P6_3/mmc$ the mirror plane perpendicular to **c** is situated at $z = 1/4, 3/4$, hence the hexagonal closest-packed oxygen layer that functions as a mirror plane has $z = 1/4, 3/4$.

(2) Due to the restriction that **O**- and $\mathbf{T}_x$-layers have to alternate, the mirror plane passing through the centers of spheres in the hexagonal closest packed layers is valid for the anions but not for the cations. Remaining allowed symmetries are hence $P3m1$, $R3m1$, $P\bar{3}m1$, $R\bar{3}m$, and $P6_3mc$, of which $P\bar{3}m1$ and $P6_3mc$ are maximal non-isomorphic subgroups of $P6_3/mmc$ (Hahn 1996).

$P\bar{3}m1$ is valid for structures with an odd sum of *S* and *N* modules (6*T*, 10*T*, 14*T*; Table 1) or, in other words, for högbomites with a number of ($4n + 2$) oxygen layers as repeat sequence. This can be explained by the fact that for "*h*" oxygen layers at $z = 1/4, 3/4$, the cations layers **O** or $\mathbf{T_2}$ are situated at the height of the inversion center, $z = 0, 1/2$, and hence the inversion center remains. Due to the uneven number of $\mathbf{T_2}$-layers it is not possible to have every $\mathbf{T_2}$-layer related to a second $\mathbf{T_2}$-layer at a distance of $z = 1/2$, as necessary for a 6_3 screw axis. For the same reason the *c* glide plane is lost. The remaining symmetry is therefore $P\bar{3}m1$.

$P6_3mc$ is valid for structures with an even sum of both *S* and *N* modules (8*H*, 12*H*, 16*H*; Table 1) or for 4*n* oxygen layers. In this case not a cation but a "*c*" oxygen layer is situated at $z = 0, 1/2$ with an **O**-layer above and a $\mathbf{T}_x$-layer below (or the other way round), causing loss of the inversion center. Due to the even number of $\mathbf{T_1}$, $\mathbf{T_2}$, and **O**-layers, each layer at a height of *z* has a corresponding layer at a height $z + 1/2$ that is related to the former via a 6_3 screw axis. The remaining symmetry of polysomes with an even sum of *S* and *N* modules is $P6_3mc$.

$R\bar{3}m$, found for the 18*R* polysome and the 24*R* polysome of högbomite and nigerite, is a minimal non-isomorphic supergroup of $P\bar{3}m1$. Rhombohedral lattices impose certain conditions on the stacking sequence (Verma and Krishna 1966). This is generally a 3*n* repetition of the closest-packed layers and specifically for högbomites a minimum number of two *N* modules (clustering of *N* modules) and one *S* module for each *n*. Hence the series of structures with a rhombohedral lattice start with $n = 3 \times (2N + 1S) = 18$ oxygen layers as repeat sequence. The clustering of *N* modules leads to the suggestion that **O**-layers sandwiched between two $\mathbf{T_1}$-layers contain hydroxyl on both sides, as found for nigerite-24*R* and högbomite-24*R* (Fig. 6).

Suggested nomenclature for högbomite- and nigerite-group minerals

A detailed description of the revised nomenclature for högbomite- and nigerite-group minerals, recently accepted by CNMMN, will be published elsewhere. Here only an overview of the revised högbomite nomenclature is presented. Högbomite-group minerals are distinguished from nigerite-group minerals by Ti > Sn. The högbomite group is classified in subgroups. In magnesiohögbomite, originally named högbomite by Gavelin (1916), the *S* module is derived from spinel $MgAl_2O_4$, in zincohögbomite (Ockenga et al. 1998) the *S* module is derived from gahnite $ZnAl_2O_4$, and in ferrohögbomite the *S* module is derived from hercynite $Fe^{2+}Al_2O_4$.

A new polysome nomenclature has been accepted by IMA CNMMN for högbomite-group minerals. To characterize the various polysomes found for each subgroup (zincohögbomite, ferrohögbomite, magnesiohögbomite) a hyphenated suffix composed of the total number of nolanite (*N*) and spinel (*S*) modules is attached. The module symbols (*N*, *S*) are italicized and given in the sequence first *N* and then *S*. The use of italicized capital letters as suffix for characterization of polysomatic building blocks has been adopted from magnetoplumbite related compounds (Kohn and Eckart 1964). Notice that each new polysome has species status and thus requires approval by CNMMN. According to this new nomenclature högbomite-10*T* and högbomite-24*R*, described in this paper, become magnesiohögbomite-2*N*3*S* and magnesiohögbomite-6*N*6*S* (Table 1). In the revised nomenclature the modeled 12*H* and 14*T* polysomes receive the new suffixes -2*N*4*S* and -2*N*5*S*, respectively.

Considering that nolanite (*N*) and spinel (*S*) modules have the idealized compositions $TM_4O_7(OH)$ and $T_2M_4O_8$, respectively, the simplified formula of each polysome can be determined by adding the modular formulas. Each module is normalized to two oxygen layers or in other words each module is 4.6 Å thick. Thus the total number of modules given in the suffix multiplied by 4.6 Å yields the length of the **c**-axis (in the hexagonal setting). Structural systematic of högbomite and nigerite-group polysomes (discussed above) has indicated that polysomes with even numbers of modules are hexagonal, while those with odd numbers of modules are trigonal. The exceptions are the rhombohedral polysomes where both the number of *N* and of *S* modules can be divided by three.

ACKNOWLEDGMENTS

Samples of högbomite were provided by A. Pring (Adelaide, Australia), M.A. Zakrzewski (Amsterdam, The Netherlands), E. Grew (Maine, U.S.A), K. Thalheim, Staatliches Museum für Mineralogie zu Dresden (Germany), G. Propach (München, Germany), M. Koelbl-Ebert, Geologische Staatssammlung, München (Germany), A. Kalt (Heidelberg, Germany). E. Gnos (Bern) kindly helped with the electron-microprobe analyses. The FTIR analysis was kindly performed by E. Libowitzky (Vienna, Austria). The Swiss Nationalfond granted financial support. Constructive reviews by D.R. Peacor and an anonymous referee are gratefully acknowledged.

REFERENCES CITED

Arakcheeva, A.V., Pushcharovskii, D.Yu., Rastsvetaeva, R.K., Kashaev, A.A., and Nadezhina, T.N. (1995) Crystal structure of nigerite-6*H*. Crystallography Reports, 40, 587–592.

Armbruster, T. (1998) Zincohögbomite-8*H* from Samos (Greece): crystal structure, polysomatism, and polytypism in högbomite related structures. Schweizerische Mineralogische und Petrographische Mitteilungen, 78, 461–468.

Armbruster, T., Bermanec, V., Zebec, V., and Oberhänsli, R. (1998) Titanium and iron poor zincohögbomite-16*H*, $Zn_{14}(Al,Fe^{3+},Ti,Mg)_8Al_{24}O_{62}(OH)_2$, from Nezilovo, Macedonia: occurrence and crystal structure of a new polysome. Schweizerische Mineralogische und Petrographische Mitteilungen, 78, 469–477.

Bermanec, V. and Šćavničar, S. (1993) Magnetoplumbite from Nežilovo, Macedonia: crystal structure refinement of zinc-rich magnetoplumbite. Neues Jahrbuch für Mineralogie Monatshefte, 1993, 481–486.

Bermanec, V., Holtstam, D., Sturman, D., Criddle, A.J., Back, M.E., and Šćavničar, S. (1996) Nežilovite, a new member of the magnetoplumbite group, and the crystal chemistry of magnetoplumbite and hibonite. Canadian Mineralogist, 34, 1287–1297.

Beukes, G.J, van Zyl, V.C., Schoch, A.E., De Bruiyn, H., and van Aswegen, G. (1986) A högbomite-spinel-gedrite-paragenesis from northern Bushmanland, Namaqua mobile belt, South Africa. Neues Jahrbuch für Mineralogie Abhandlungen, 155, 53–66.

Bovin, J. (1981) High resolution transmission electron microscopy of minerals: defects and new combination structures in the högbomite group. Geologiska Foereningen i Stockholm Foerhardingar, 103, 122–124.

Brown, I.D. (1996) VALENCE: a program for calculating bond valences. Journal of Applied Crystallography, 29, 479–480.

Bruker AXS (1997) XPREP Ver. 5.1: a program for reciprocal space exploration. Bruker Analytical X-ray Systems, Madison, WI 53719-1173.

Bruker AXS (1999) SAINT+ Ver. 6.01/NT: a program for reduction of raw crystallographic data frames taken with Siemens area detectors. Bruker Analytical X-ray Systems, Madison, WI 53719-1173.

Burke, E.A.J. and Lustenhouwer, W.J. (1981) Pehrmanite, a new beryllium mineral from the Rosendal pegmatite, Kemiö Island, southwestern Finland. Canadian Mineralogist, 19, 311–314.

Chen, J., Shi, Y., Pan, Zh., and Zhizhong, P. (1989) The crystal structure and crystal chemistry of a new mineral, pengzhizongite-6H. Earth Science Journal of Wuhan College of Geology, 14, 413–422.

Curien, H., Guillemin, C., Orcel, J., and Sternberg, M. (1956) La hibonite, nouvelle espèce minérale. Compte Rendus Hebdomadaires des Seances de l'Academie des Sciences, 242, 2845–2847.

Ding, K., Sheng, G., and Wang, C. (1982) Discovery and study of 6*H*-nigerite. Yankuang Ceshi, 1, 30–35.

Enraf, N. (1983) Structure determination package (SDP). Enraf Nonius, Delft, The Netherlands.

FCGEN (1998) Program for calculation of structure factors. Laboratory for Crystallography, University of Bern, Switzerland.

Friedman, G.M. (1952) Study of högbomite. American Mineralogist, 37, 600–608.

Gatehouse, B.M. and Grey, I.E. (1982) The crystal structure of högbomite-8H. American Mineralogist, 67, 373–380.

Gatehouse, B.M., Grey, I.E., and Nickel, E.H. (1983) The crystal chemistry of nolanite, $(V,Fe,Ti,Al)_{10}O_{14}(OH)_2$, from Kalgoorlie, Western Australia. American Mineralogist, 68, 833-839.

Gavelin, A. (1916) Über Högbomit. Bulletin of the Geological Institution of the University of Uppsala, 15, 289–316.

Grew, E.S., Abraham, K., and Medenbach, O. (1987) Ti-poor hoegbomite in kornerupine-cordierite-sillimanite rocks from Ellammankovilpatti, Tamil Nadu, India. Contributions to Mineralogy and Petrology, 95, 21–31.

Grey, I.E. and Gatehouse, B.M. (1979) The crystal structure of nigerite-24R. American Mineralogist, 64, 1255–1264.

Grey, I.E., Velde, D., and Criddle, A.J. (1998) Haggertyite, a new magnetoplumbite-type titanate mineral from the Prairie Creek (Arkansas) lamproite. American Mineralogist, 83, 1323–1329.

Göbbels, M., Woermann, E., and Jung, J. (1995) The Al-rich part of the system CaO-Al_2O_3-MgO. I: Phase relationships. Journal of Solid State Chemistry, 120, 358–363.

Göbbels, M., Kimura, S., and Woermann, E. (1998) The Aluminium-rich part of the system BaO-Al_2O_3-MgO. I: Phase relationships. Journal of Solid State Chemistry, 136, 253–257.

Haggerty, S.E., Grey, I.E., Madsen, I.C., Criddle, A.J., Stanley, C.J., and Erlank, A.J. (1989) Hawthorneite, $Ba[Ti_3Cr_4Fe_4Mg]O_{19}$: A new metasomatic magnetoplumbite-type mineral from the upper mantle. American Mineralogist, 74, 668–675.

Hahn, T., Ed. (1996) International Tables for Crystallography, Volume A: Space Group Symmetry. Kluwer Academic Publishers, Dordrecht, The Netherlands.

Iyi, N., Inoue, Z., and Kimura, S. (1986) The crystal structure and cation distribution of highly nonstoichiometric magnesium-doped potassium β-alumina. Journal of Solid State Chemistry, 61, 236–244.

Iyi, N., Takekawa, S., and Kimura, S. (1989) Crystal chemistry of hexaaluminates: β-alumina and magnetoplumbite structures. Journal of Solid State Chemistry, 83, 8–19.

Iyi, N., Göbbels, M., Matsui, Y. (1995) The Al-rich part of the system CaO-Al_2O_3-MgO. II: Structure refinement of two new magnetoplumbite-related phases. Journal of Solid State Chemistry, 120, 364–371.

Iyi, N., Göbbels, M., and Kimura, S. (1998) The aluminium-rich part of the system BaO-Al_2O_3-MgO. II: Crystal structure of the β-alumina-related compound, $Ba_2Mg_6Al_{28}O_{50}$. Journal of Solid State Chemistry, 136, 258–262.

Kato, K. and Saalfeld, H. (1968) Verfeinerung der Kristallstruktur von $CaO{\cdot}6Al_2O_3$. Neues Jahrbuch für Mineralogie Abhandlungen, 109, 192–200.

Kohn, J.A. and Eckart, D.W. (1964) Stacking relations in the hexagonal ferrites and a new series of mixed-layer structures. Zeitschrift für Kristallographie, 119, 454–464.

Kojima, H. (1982) Fundamental properties of hexagonal ferrites with magnetoplumbite structure. Ferromagnetic Materials, 3, 305–391.

Kunz, M. and Brown, D. (1995) Out-of-center distortions around octahedrally coordinated d^0 transition metals. Journal of Solid State Chemistry, 115, 395–406.

Kummer, J.T. (1972) β-alumina electrolytes. Progress in Solid State Chemistry, 7, 141–175.

Lengauer, C.L., Tillmanns, E., and Hentschel, G. (2001) Batiferrite, $Ba[Ti_2Fe_{10}]O_{19}$, a new ferrimagnetic magnetoplumbite-type mineral from the Quarternary volcanic rocks of the western Eifel area, Germany. Mineralogy and Petrology, 71, 1–19.

McKie, D. (1963) The högbomite polytypes. Mineralogical Magazine, 33, 563–580.

Medenbach, O. (1986) Ein modifiziertes Kristallbohrgerät nach Verschure (1978) zur Isolierung kleiner Einkristalle aus Dünnschliffen. Fortschritte der Mineralogie, 64 Beiheft 1, 113.

Moore, P.B., Gupta, P.K.S., and Le Page, Y. (1989) Magnetoplumbite, $PbFe_{12}O_{19}$: refinement and lone-pair splitting. American Mineralogist, 74, 1186–1194.

Neiva, A.M.R. and Champness, P.E. (1997) Nigerite and gahnite from the granitic pegmatite veins of Cabanas, Ponte do Lima, northern Portugal. Neues Jahrbuch für Mineralogie Monatshefte, 1997, 385–409.

Nel, H.J. (1949) Hoegbomite from the corundum fields of the eastern Transvaal. Union of South Africa, Geological Survey Memoir, 43, 1–7.

Nuber, B. and Schmetzer, K. (1983) Crystal structure of ternary Be-Mg-Al oxides: taaffeite, $BeMg_3Al_8O_{16}$, and musgravite, $BeMg_2Al_6O_{12}$. Neues Jahrbuch für Mineralogie Monatshefte, 1983, 393–402.

Ockenga, E., Yalçin, Ü., Medenbach, O., and Schreyer, W. (1998) Zincohögbomite, a new mineral from eastern Aegean metabauxites. European Journal of Mineralogy, 10, 1361–1366.

Patterson, A.L. and Kasper, J.S. (1959) Close Packing. In J.S. Kasper and K. Londsdale, Eds., International Tables for X-ray Crystallography, Vol. II Mathematical Tables, p. 342–354. The Kynoch Press, Birmingham.

Peacor, D.R. (1967) New data on nigerite. American Mineralogist, 52, 864–866.

Petersen, E.U., Essene, E.J., Peacor, D.R., and Marcotty, L.A. (1989) The occurrence of högbomite in high-grade metamorphic rocks. Contributions to Mineralogy and Petrology, 101, 350–360.

Pouchou, J.L. and Pichoir, F. (1991) Quantitative analysis of homogeneous or stratified microvolumes applying the model "PAP". In K.F.J. Heinrich and D.E. Newbury, Eds., Electron probe quantitation, p. 31–75. Plenum Press, New York

Sheldrick, G.M. (1997a) SHELXS-97. A program for crystal structure determination. University of Göttingen, Germany.

———(1997b) SHELXL-97. A program for crystal structure refinement. University of Göttingen, Germany.

Schmetzer, K. and Berger, A. (1990) Lamellar iron-free högbomite-24*R* from Tanzania. Neues Jahrbuch für Mineralogie Monatshefte, 1990, 401–412.

Schumacher, J.C., Schäfer, K., and Seifert, F. (1987) Lamellar nigerite in Zn-rich spinel from the Falun deposit, Sweden. Contributions to Mineralogy and Petrology, 95, 182–190.

Shubnikov, A.V. and Koptsik, V.A. (1974) Symmetry in Science and Art, p. 219–223. Plenum Press, New York.

Teale, G.S. (1980) The occurrence of högbomite and taaffeite in a spinel-phlogopite schist from the Mount Painter Province of South Australia. Mineralogical Magazine, 43, 575–577.

Verma, A.R. and Krishna, P. (1966) Polymorphism and Polytypism in Crystals, p. 154–162. Wiley, New York.

Zakrzewski, M.A. (1977) Högbomite from the Fe-Ti deposit of Linganga (Tanzania). Neues Jahrbuch für Mineralogie Monatshefte, 1977, 373–380.

MANUSCRIPT RECEIVED FEBRUARY 6, 2001
MANUSCRIPT ACCEPTED SEPTEMBER 21, 2001
MANUSCRIPT HANDLED BY MARK WELCH